A NEW DESIGN OF EXCITATION MECHANISM TO BE EXPLOITED BY MODERN RF EXCITED CO_2 LASERS

A THESIS SUBMITTED TO
THE GRADUATE SCHOOL OF NATURAL AND APPLIED SCIENCES
OF
MIDDLE EAST TECHNICAL UNIVERSITY

BY

R. SALUR KURUCU

IN PARTIAL FULFILLEMENT OF THE REQUIREMENTS
FOR
THE DEGREE OF MASTER OF SCIENCE

IN

PHYSICS

AUGUST 2004

Approval of the Graduate School of Natural and Applied Sciences

_____

Prof. Dr. Canan ÖZGEN
Director

I certify that this thesis satisfies all the requirements as a thesis for the degree of Master of Science.

_____

Prof. Dr. Sinan BİLİKMEN
Chair of Physics Department

This is to certify that we have read this thesis and that in our opinion it is fully adequate, in scope and quality, as a thesis for the degree of Master of Science.

_____

Assoc. Prof. Dr. Akif ESENDEMİR
Supervisor

Examining Committee Members

Prof. Dr. İbrahim GÜNAL	METU	_____
Assoc. Prof. Dr. Akif ESENDEMİR	METU	_____
Assoc. Prof. Dr. Mehmet PARLAK	METU	_____
Assoc. Prof. Dr. Serhat ÇAKIR	METU	_____
Dr. Ali ALAÇAKIR	TAEK	_____

I hereby declare that all information in this document has been obtained and presented in accordance with academic rules and ethical conduct. I also declare that, as required by these rules and conduct, I have fully cited and referenced all material and results that are not original to this work.

Name, Last name :

Signature :

ABSTRACT

A NEW DESIGN OF EXCITATION MECHANISM
TO BE EXPLOITED BY MODERN RF EXCITED CO_2 LASERS

KURUCU, R. SALUR
M.S., Department of Physics
Supervisor: Assoc. Prof. Dr. Akif Esendemir

August 2004, 105 pages

On this thesis work, design and construction of an up to date complete RF excitation system was intended. This excitation system is mainly based on highly efficient switching power generators and proper coupling of the power to the object plasma. This new excitation system design should answer the demands of today's progressed CO_2 lasers on various power ranges. Though it could be used by a large variety of applications including RF plasma and RF heating, on the first occasion in order to define design considerations, this system is to be exploited by RF excited fast flow and RF excited slab CO_2 laser constructions.

Keywords: CO_2 Laser, RF power generators, RF excitation, RF pumping of laser, class-e amplifiers, capacitive RF discharges, capacitively coupled RF plasma, switch mode amplifiers.

ÖZ

MODERN RF UYARIMLI CO_2 LASERLER İÇİN YENİ BİR UYARIM MEKANİZMASI TASARIMI

KURUCU, R. SALUR
Yüksek Lisans, Fizik Bölümü
Tez Yöneticisi: Doç. Dr. Akif Esendemir

Ağustos 2004, 105 sayfa

Bu tez çalışmasında tam ve güncel bir radyo frekans uyarım sisteminin tasarlanıp oluşturulması amaçlanmıştır. Söz konusu sistem temelde yüksek verimlilikteki anahtarlamalı güç üreteçleri ile üretilen gücün hedef plazma ortamına uygun şekilde aktarılabilmesi sorunlarının çözümlenmesine dayanmaktadır. Bu yeni uyarım sistemi, günümüzün gelişmiş CO_2 laserlerinin çeşitli güç dilimlerindeki ihtiyaçlarını karşılayacaktır. Anılan sistem RF ısıtma ve RF plasma gibi çok çeşitli uygulamalarda kullanılabilecektir ancak tasarımın kıstasları belirlenirken ilk sefer için RF uyarımlı hızlı eksensel akışlı CO_2 ve RF uyarımlı levha CO_2 laserlerinde faydalanılması düşünülmüştür.

Anahtar Kelimeler: CO_2 Laseri, RF güç üreteçleri, RF uyarım, RF pompalama, sınıf-E amplifikatör, kapasitif RF deşarj, kapasitif RF plasma, anahtarlamalı amplifikatör.

ACKNOWLEDGEMENTS

I would like to thank following people for their continuos support, encouragement and their special efforts to keep their belief on me;

Oğuz Kurucu, Ali Alaçakır, Akif Esendemir, Sinan Bilikmen, Sevim Kurucu, Nermin Tanyeri, Selis Bağdat, Iulian Gutu, Ebru Tümer, Gökhan Aykaç, Zeynep Tangün, Barçın Kurucu, Orkun Kurucu, Suna Yalaz, Özgür Öğret, Sanem Karaçelik, Eray Özkural.

TABLE OF CONTENTS

LIST OF TABLES

TABLE

LIST OF FIGURES

FIGURES

CHAPTER 1

INTRODUCTION

This experimental research work aims to develop Radio Frequency Generator Device, which will ignite and maintain discharge plasma of a certain gas mixture at moderate pressures to be exploited within the active medium of CO_2 laser. The proposed device is an adaptive system that makes use of proper RF (radio frequency) energy on any of the varying conditions, to keep the plasma on a steady state. The RF energy is coupled into the plasma capacitively. This proposed device is demanded to be relatively cheap with its building components, easier to construct, reliable, durable and safe on usage. These expectations can be only be satisfied simultaneously with the simplest design that is possible.

Plasma is a partially ionized gas. This state of matter was first identified by Sir William Crookes in 1879, and dubbed "plasma" by Irving Langmuir [1]. Plasma can be broadly divided into "thermal" and "cold" varieties. Cold plasma, which is the primary interest of this study, is one where only a small fraction of the atoms in a gas are ionized, and the electrons reach a very high temperature, whereas the ions remain at the ambient temperature.

Using electric field to accelerate electrons, which ionize the atoms, can create such plasma. The electric field is either capacitively or inductively coupled into the gas. On the case of capacitive coupling of RF energy, oscillating potential field from the electrodes is applied to the medium of interest. Electrodes are possible to be coated with some other dielectric material or can be outside the subject chamber. Capacitively coupled RF excitation is not the sole way to create plasma for the

desired application, but it might be the most successful means to create and to benefit, to be discussed among the following chapters.

Although the RF excited plasma has a large variety of applications, apart from some rare used applications, three of them are the popular interests of the theme "CCD" (capacitively coupled discharges) on which the discussions on this work are narrowed. On the low-pressure range p ; $1-10^{-3}$ Torr; there are the industrial and scientific activities of "etching" and "thin film deposition". For the moderate pressures of p ; $1-100$ Torr; widely used application is the excitation of the active laser medium, primarily the CO_2 lasers.

RF CCD was first used in the 1960s to obtain active medium for He-Ne and CO_2 lasers [2] [3]. Nevertheless RF excited lasers were not successful at that time. The physics behind the RF CCD were not clear, else the DC excitation was preferable not requiring complex devices or load coupling.

Combinations of DC (direct current) and RF excitations have gained very much success after 1970s [4], though trials of RF excitation alone were still not successful. During the 1980s after intensive studies and empirical work, RF excitation of the CO_2 lasers, have been promising [5], and then commercially produced on the following years.

On many circumstances, ignition and maintenance of CDD may reach current densities up to 0.1A/m^2 and requires powerful RF generators of a few to several hundreds of kW. For the scientific research usually so-called "self excited tube generators" are used. Although these are quite reliable and easy to build and maintain, their commercial usage is no more valid. They are inefficient, fragile and require very large volumes of space. It is necessary to cool them with great efforts.

However modern power conversion technology continuously seeks for techniques for devices that are more efficient, safe, reliable, and more durable on harsher ambiences, easy to maintain, compact and complete on the least possible volume and weight. Extended lifetime of operation, power factor correction, satisfaction of international standards, regulations and safety considerations are some of the other expectations of the industry.

Impedance matching and current control are other demands of CCD systems to be asked. Plasma could be created maintained and exploited on some very strict ranges of operational parameters especially of the frequency, voltage, current and gas temperature. Although the plasma is fed very well with power it might be on a state that is not useful or the plasma may be over heated which will lead to the disassociation of the molecular gas, the CO_2 on many circumstances. The useful active medium of any CO_2 laser should always be kept well below 600K [8].

After the availability of solid state MOSFETs, which are cheap and capable of handling large currents with in the range thousands of volts on RF frequencies, they are naturally on the scope of thesis work. There are at least three positions on such a system that any designer would like to benefit MOSFETs.

Obtaining an appropriate active medium and extraction of the optical power out of this medium efficiently and on a certain beam quality are the two major problems of the laser design. Alternative solutions to the former problem will have its outcomes for the design and construction of more advanced lasers that are very much compact, easy to apply, efficient for the maintenance costs, cheap, durable and reliable. Quest for these solutions is also the motivation point for this thesis work.

Through the 2nd chapter, dynamics for the plasma of the related gas mixture will be made clearer. A better understanding of the plasma behavior and characteristics will reveal the demands from the system to be proposed.

The 3rd chapter will clarify the building blocks of such a system. Criteria for the selection and design of a particular building block will be explained. After the determination of the operation specific parameters, there will be a complete picture of the whole system by the end of the chapter.

The 4^{th} chapter will contain information on the practical implementation of the particular building blocks and of the experiments carried out. Experimental data and the notes worth attention about the observations and experimental experience will be given through this chapter. Details about the calculations of some parameters will take place on appendices.

Finally the 5th chapter will deduce the consequences. Results from the experiments and the outcomes of the research will be discussed. This chapter will end with a new list of problems to overcome and new objectives for the future work.

CHAPTER 2

ACTIVE MEDIUM OF CO_2 LASERS WITH RADIO FREQUENCY CAPACITIVE DISCHARGES

During the design process of a CO_2 laser, some design constraints associated with the discharge characteristics determine the size and geometry of the usable volume available for the active medium. These criteria may result from issues, such as expectations from the output beam or any other geometrical considerations as in the case of waveguide lasers or annular ones. In any case it is quite natural to demand the most possible gain from a given volume of active medium. In order to provide this one may raise the pressure and feed as much power as could be possible. Nevertheless there is a limit.

2.1 Active Medium of the CO_2 Laser

Regarding the conventional classifications, CO_2 lasers are molecular gas lasers. The active medium of a CO_2 laser is composed of a gas mixture; in general case CO_2 and N_2 molecules and atomic Helium. CO_2 is the molecule of the primary importance of which the so-called “population inversion” is expected. There may exist some supplementary gases such as Xe or water vapor with various effects to be exploited on varying the chemical or the physical properties of the medium.

2.1.1 Excitation of the active medium of CO2 Laser

On 1961 J.C. Polanyi explained the possibility of using molecular vibrations to be useful for laser operations [6]. Afterwards C.K.N. Patel described the laser action from the vibrational-rotational transitions of CO_2 molecule in a discharge [7].

2.1.1.1 Excitation of CO_2 Molecule

CO_2 is a linear, symmetric, triatomic molecule with the carbon atom balanced against the two oxygen atoms, O-C-O. Oxygen atoms covalently bonded to a central carbon atom. Although CO_2 is a triatomic molecule, it behaves much like a simple diatomic molecule because its structure is linear. Such a linear triatomic molecule has three normal modes of vibration. The molecule has two stretching vibrational modes, labeled ν_1 and ν_3 and a bending mode; ν_2-l. l is the quantum number for vibrational angular momentum. ν_1 is the number associated with the symmetrical stretching of the molecule. ν_2 is that associated with bending and ν_3 with asymmetrical stretching. Since the molecules do not have fixed orientations within, they tend to vibrate [8].

They are able to rotate and spin because they are in a gaseous state. These vibrational and rotational states, as in electronic states, are quantized.

Transitions between vibrational energy states results in photon emission in the infrared, while transitions between rotational states emit photons in the microwave region. Members of the same vibrational state are distributed amongst available energy levels as determined by Boltzmann statistics and are in thermal equilibrium. CO_2 molecule vibrates on all of these three states.

The complete state is described by three integers (nmq). (001) to (100) and (001) to (020) are the most important energy level transitions allowing emissions of 10.4 um and 9.4 um respectively. When the laser is operative, the (100) mode and its chain become heavily populated. This chain cannot radiate to the ground state and can only radiate weakly to the lower bending modes. The (100) and (020) vibrational

levels depopulate rapidly. Since the infrared transitions are relatively slower than this depopulation, a population inversion is achieved.

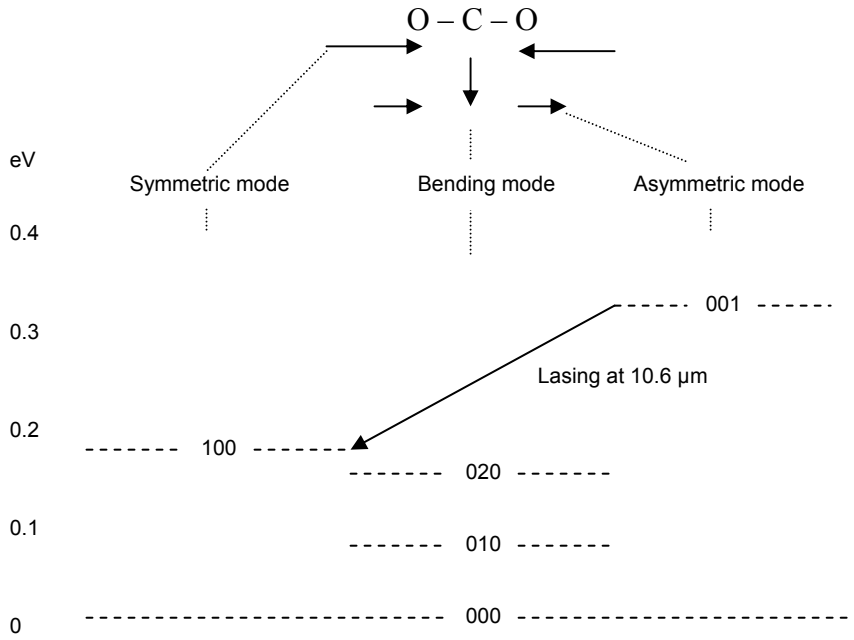

Fig 1. Vibrational modes and energy levels of CO_2 molecule

2.1.1.2 Gas Composition of CO_2 Laser Active Medium

Although very first CO_2 lasers were utilizing pure CO_2 as an active medium, reasonable powers were not obtainable. CO_2 molecule was inefficient to be excited by direct electron collisions. On 1964 N_2 is used to obtain more efficient lasing from CO_2 [3]. CO_2 molecules were being excited through collisions with previously excited N_2 molecules.

This transfer of energy occurs by a resonant effect. Since the lowest vibrational energy level of the symmetric molecule N_2 is metastable and cannot radiate. However it has energy very close to that of the first energy level of the asymmetric stretch mode of CO_2 at about 2 meV with in the thermal energy spread of

25 meV. Thus N_2 molecules are able to transfer their energy and excite the CO_2 molecules very efficiently. Then after, excitation mechanism exploiting N_2 molecules at useful partial pressure inside the active medium of any CO_2 laser has become a convention.

Laser theory states that, maintenance of the population inversion, which is critical for any lasing activity, are dependent on fast decay of the lower energy levels of the any given active medium element. The two lower laser levels on the CO_2 energy scheme are (020) and (100).

Addition of He to the active medium of a CO_2 laser is beneficial to induce fast decay of these two levels (020) and (100), besides He is also effective on depopulation of the lowest (010) bending mode as well. This is also of the great importance, that is, (010) mode will again be useful on relaxation of the lower laser levels of (020) and (100) since, (010), (020), and (100) levels are all strongly coupled together through resonant collisions. However He is not effective on depopulation of the useful (001) excitation level. The low mass of He makes it effective in trading its kinetic energy with the molecule internal energy modes for small energy changes.

Besides He is effective on the maintenance of the active medium. It increases the thermal conduction with the cavity, which in turn keeps the temperature low, the Doppler width small and the gain high.

CO_2	**N_2**	**He**	**Laser Power Rating W**
1	3	17	20
1	1.5	9.3	50
1	1.5	9.3	100
1	1.35	12.5	275
1	8	23	375
1	6.7	30	525
1	2.3	17	1000

Table 1. Typical gas composition ratio of CO_2 Lasers [21]

There might be some additions to this very standard gas mixture of the CO_2 lasers for some other particular reasons. Maintenance aspects of the steady state operation of such a laser often suffer from the disassociation phenomena of the CO_2 molecule in to the oxygen and CO. Disassociation of CO_2 decreases the usable ratio of CO2 inside the system. Addition of CO or O_2 may be considered on a particular laser design in order to limit the disassociation, working against it on the chemical equilibrium. Some other types of catalytic, such as water or H_2 can also be exploited as additives in order to overcome this problem. Water vapor has also known to have a large effect on relaxation of the upper excited levels [8].

Finally, sometimes Xe is found in the gas mixtures of the CO_2 lasers. Up to 60% of the electrical input power can be stored in vibrational energy of N_2 at an optimal electron temperature of about 12.000 K [9]. Nevertheless most of the times this temperature tend to come to a is higher value during continuos operations, leading to the loss of efficiency for the system. The designer may benefit the addition of an approximate relative pressure of 0.5% Xe, in order to lower the electron temperature to a more optimal value within the active medium. Although the underlying mechanism is rather more complicated and it has negligible effects on discharge parameters and is beyond the scope of this study.

2.1.1.3 Pressure and Temperature Considerations

Another aspect of the maintenance of the active medium of the essential importance for the lasing process of CO_2 is the gas temperature in the plasma. Without an effective gas cooling, high laser efficiency cannot be reached. Although theoretical quantum efficiencies of the CO_2 lasers are about 40% [8], practical lasers usually have efficiencies well bellow 20%. Remaining at least 80% of the input energy is dissipated on electrical power change in to heat, to the heating of the gas mixture of the active medium.

However a temperature above 600 K inside the cavity is damaging to the laser generation [8]. On practical considerations of the CO_2 laser design, providing an effective heat removal is often the primary constraint to be considered. The heat

may be removed via heat conductivity to the walls of the discharge chamber (diffusional cooling), or the heat is removed from the chamber by a fast flow of laser mixture through it. First one is sufficient and effective for small and moderate power lasers. The second one is commonly used in high power lasers.

Heat will destroy the gain vs. input power proportionality with an indirect mechanism. The excess heat will increase the disassociation rate of the CO_2 molecules and the system suffers not only from the lack of CO_2 in the active medium but also the CO molecules joined the system will absorb energy to radiate useless photons. Thus temperature of the active medium is often limits the average power in to the system.

Pressure on the other hand can be related with laser gain as stated before; the laser output power will increase with the raised pressure up to critical value. Since still increased power means more power input again temperature rise is an important factor for the pressure up limit.

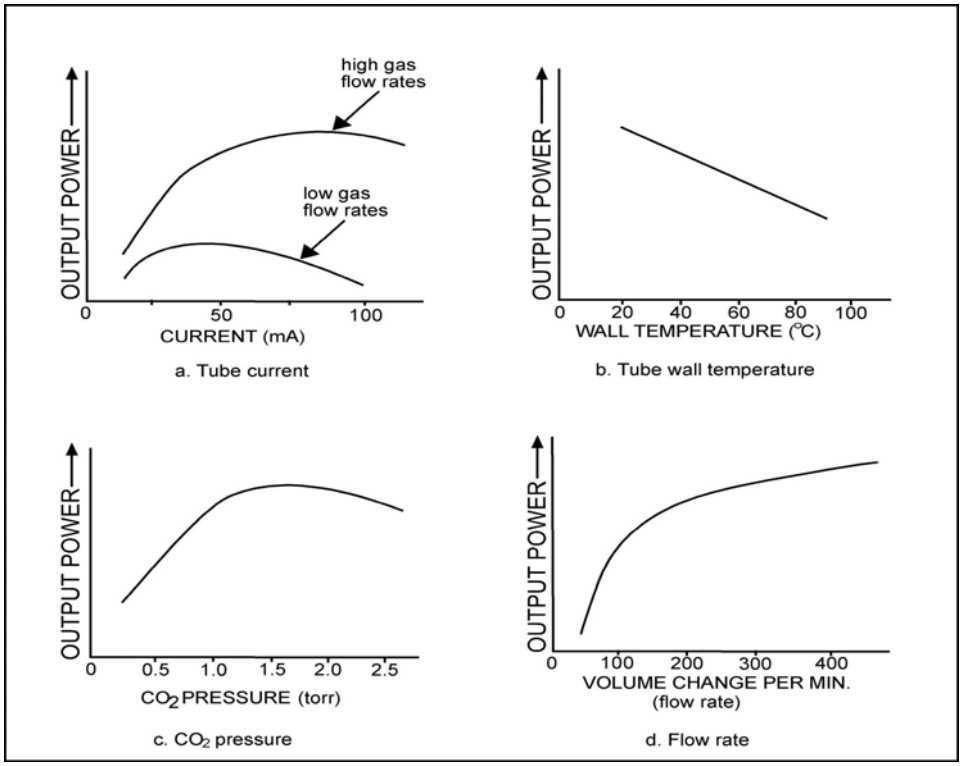

Fig 2. Typical effects of temperature related parameters on laser power [21]

Plasma characteristics are also directly affected by the pressure parameter. The product of the discharge gap size and the pressure value, " pd " is one of the important determining factor of the plasma characteristics inside the active medium volume, strongly related to the current-voltage behavior.

Thus for any group of given laser parameters there is an optimal "*pd*" value. On the contrary of the active medium temperature, it is a cleaver choice to keep the pressure parameters variable during the design process of a CO_2 laser. It is of the common practice to stick on moderate pressures " p ; $1-100$ Torr" for any CO_2 laser, apart from the ones especially designed to operate with high pressures, such as TEA CO_2 lasers operating only on pulsed regimes, which are out of the scope of this thesis work.

2.1.2 Types of CO_2 Laser

The main challenge on CO_2 laser engineering is to obtain maximum power output power from the smallest volume possible, with better efficiency and beam quality an in a cost effective design. Also some particular applications may ask for some other specifications of their own such as pulse duration or increased lifetime. Different solutions to these demands create better results for some aspects, while ignoring much or less of some others. There is no optimal CO_2 laser to satisfy all the demands together but there are many types of CO_2 lasers, each of one might be satisfactory for a specific application.

2.1.2.1 Heat Removal Considerations

Heat removal considerations are one of the primary criteria leading to these classifications of the CO_2 laser types. The gas mixture medium in a CO2 laser is cooled either by convection and thermal diffusion to the walls of the chamber or fast removal or recycling of the gas mixture.

Diffusion cooled conventional tube lasers on which the laser gas mixture is flowing slowly on longitudinal direction have their approximate limit of 50W of optical power output per unit meter of the tube length. This value is not depended on the excitation mechanism, optical system used or to the tube diameter but only from heat removal reasons.

It is demonstrated, that is possible to create high power diffusion cooled lasers by using different geometrical arrangements. These types of diffusion-cooled lasers are called “slab CO2 lasers” [10]. Essential advantages of this type of lasers are a compact design and a high laser output power. Slab lasers are one of the basic motivations of RF excitation since they are not easy to excite with DC discharge. Slab lasers are convenient for all-metal designs where no other fragile parts are used. However, when output powers beyond 1kW are intended, then so called “fast flow” lasers are reasonable, even though they have serious engineering difficulties [11]. These lasers make use of the laser gas mixture that is flowing very fast on the system. Apart from the active medium, gas mixture flows through a chiller system where it is reconditioned for proper operation. There are two common types of fast flow CO_2 lasers according to the direction of flow; “fast transverse flow” and “fast axial flow”. Fast axial flow CO_2 lasers require folded designs to increase the power after a certain value of tube length since longer tubes makes the fast flow harder. For the transverse flow case, on which the gas mixture is leaving the active medium very fast from the transverse direction, possibly one of the most effective ways of achieving high power on a relatively compact design. Nevertheless poor beam quality is the draw back of these classes of lasers [12].

2.1.2.2 Optical Considerations

A laser cavity with optical properties, other than hosting the active medium, can be fruitful. The waveguide laser is an efficient way to produce a compact CO_2 laser. It consists of, two transverse RF electrodes separated by insulating sections that form a bore region. The lateral dimensions of the bore are a few millimeters, which propagates the beam in “waveguide mode”. The tube is normally sealed with a

gas reservoir separate from the tube itself. The small bore allows high-pressure operation and provides rapid heat removal; both of which lead to high gain and high power output from a compact unit. However, for the reasons to be explained on the next section, RF excited waveguide lasers accept RF energy at very high frequencies at about a hundred MHz [13].

It is also possible to classify CO_2 lasers according to the resonator types they utilize, especially if they are not of the regular type. “Unstable resonator” slab lasers are of the great importance since they are candidates to dominate many application fields. “Plasma resonator” CO_2 laser can be another example, though they are not common for industrial applications.

2.1.2.3 Excitation Mechanism

It is possible to excite (pump) the active medium for CO_2 lasers by means of direct current “DC”, alternative current “AC”, high frequency “HF”, radio frequency “RF” and finally with microwaves. However AC and microwave excitation is not used in common whilst the latter is promising in many ways and now can operate on quasi-continuous regimes with an acceptable efficiency. Combinations of these might be used either, as in the case of the utilization of RF and DC together on “fast axial flow CO_2 lasers” which is of the common practice.

Generally speaking DC excitation is a more favorable excitation method since it is cost effective, easier to produce, with a better-known behavior and is the one with the highest efficiency of all. Nevertheless when it is the question of being compact, DC excitation is not easy to utilize on any cavity geometry. Similarly, DC excitation may suffer from the phenomena “contraction” when high powers are necessary [13]. Especially in the case of fast flow CO_2 lasers on which heat removal is not the binding factor any more, contraction effect determines the upper limit of the power to be applied.

HF operations of lasers are proven to resemble the RF operation and are obviously advantageous for being cost effective. HF operation is possible on

frequencies lower than 1MHz, down to 400kHz, with a special type of plasma regime called silent discharge [14] [9].

RF discharges, the main theme of thesis will be discussed in detail among the following sections.

Although the DC type may have some technical problems due to the great difference between the breakdown and steady-state voltages, the pulse mode lasers are possible with all these types of excitation. However, the name "pulsed mode laser" is given after some specific types, all of which can only operate on pulse regime due to their active medium properties. For instance, the "*pd"* parameter on an active medium of a TEA CO_2 is so high that steady state glow discharges are not possible [15]. Steady state operation is difficult to maintain on some other examples due to the over heating of the laser gas mixture, as in the case of microwave operation. Besides occasionally the application may demand the pulse mode operation of each type where the pulse duration and repetition rates become critical.

2.1.2.4 Cavity Geometry

Some of the CO_2 lasers are named due to their geometrical properties. Besides the slab, waveguide and capillary geometry, "folded" or "multi-channel" types are constructed to raise the achievable power on single beam of laser. Likewise "triangular" geometry is used to obtain folding, on more compact designs. Some other types can be useful for better excitation and increasing the useful volume of the active medium, taking the advantages of their geometry as in the case of "annular CO_2 lasers".

2.2 Properties of Moderate Pressure RF Capacitive Discharges

Active medium for the CO_2 lasers are usually maintained at moderate pressures p ; $1-100$ Torr. At this pressure range CCD plasma is able to appear on several different forms. All of these forms have their completely different behaviors

depending on the parameters of the cavity; electrode separation "*d*", pressure "*p*", frequency of the field applied "ω", current "*I*" and potential "*V*".

2.2.1 Optimum Power Coupling at Moderate Pressures

The effective collision frequency "υ_c" parameter of the active medium possesses key role for the explanation of many the discharge specifications. It appears on the basic equation for the velocity and displacement of a single electron inside the active medium. The principal equation governing the electron motion inside the cavity is expressed as,

$$m\dot{v} = -eE_a \sin \omega t - mv\upsilon_c \tag{2.1}$$

Followed by the force term due to the field, the second term on the right side is for the loss of the electron momentum due to the scattering of electrons by atoms or molecules. The υ_c parameter may be explained further with the relation,

$$\upsilon_c = N \overline{v} \sigma_c \tag{2.2}$$

where "*N*" is the density of atoms,"$\overline{v}$ "is the mean random velocity of an electron and "σ_c" corresponds to the transport cross section [13]. A very basic outcome of this equation is the electron collision frequency is directly proportional to the pressure of the active medium.

For the moderate pressure case where $\upsilon_c >> \omega$, very frequent collisions are expected. Then two important approximations for the solution of (2.1) are now reasonable. Firstly the electron velocity can be accounted to have the same drift velocity as, as if it is in a DC field, for a given instantaneous field amplitude; $v \approx v_d$. The drift velocity of the electron is given as,

$$v_d = \mu_e E_{0p} \tag{2.3}$$

where E_{0p} is the plasma field amplitude to be discussed later on. Second the amplitude of displacement is likely to be,

$$x = \frac{\mu_e E_a}{\omega} \cos \omega t \tag{2.4}$$

where E_a is the applied field and μ_e is the electron mobility given with the equation,

$$\mu_e = \frac{e}{m\upsilon_c} \tag{2.5}$$

and the applied field is,

$$E = E_a \sin \omega t \tag{2.6}$$

Exploiting these kinematic properties of the electron inside the active medium and the basic power definition, it is possible to calculate the mean power of a single electron to be transferred to the plasma with collisions;

$$p = \frac{dW}{dt} = \frac{F_e dx}{dt} = eE_0 \sin(\omega t)\frac{dx}{dt} \tag{2.7}$$

and power term for a single electron is multiplied with electron density n_e.

$$\bar{P} = n_e \times \int_0^T p dt = \frac{e^2 n_e E_0^2}{2m} \frac{\nu_c}{(\omega^2 + \nu_c^2)} \tag{2.8}$$

Here, the electrostatic energy can be used for substitutions,

$$\bar{U} = \frac{1}{2}\varepsilon_0 E^2 = \frac{1}{T}\int_0^T U dt = \frac{1}{T}\int_0^T \frac{1}{2}\varepsilon_0 E_0^2 \sin(\omega t) dt = \frac{1}{4}\varepsilon_0 E_0^2 \tag{2.9}$$

$$\bar{P} = \bar{U}\frac{2\omega_p^2 \nu_c}{(\omega^2 + \nu_c^2)} = \bar{U}\nu^* \tag{2.10}$$

where "ω_p" is the plasma frequency basically dependent on the electron density "n_e" and "ν^*" is the energy transfer frequency. Finally for the optimum energy transfer at a fixed frequency, one can solve for a maxima;

$$\frac{d\nu^*}{d\nu_c} = \frac{2\omega_p^2}{(\omega^2 + \nu_c^2)}(\omega^2 - \nu_c^2) = 0 \Rightarrow \omega = \nu_c \tag{2.11}$$

For $\upsilon_c >> \omega$, a large number of collisions take place within a wave period, so that the electrons are unable to build-up their steady-state oscillation energy.

This reduction in the energy acquired by the electrons between collisions is compensated for by an increase in the electric field strength. In the other limit $\upsilon_c << \omega$, the collisions are few and far between, so that many cycles of the wave period go by before a collision occurs. Thus the power absorption is not optimized and the field strength again rises.

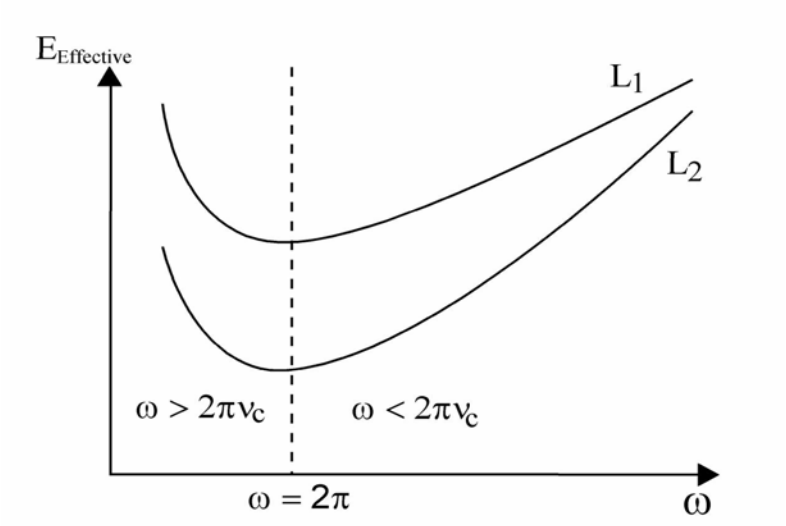

Fig 3. Effective field vs. field frequency

It may also be noted that the electrical power loss in a resistor is also due to collisions and so one may regard the condition $\omega \approx \upsilon_c$ to be similar to the impedance matching condition for maximum power transfer in RF the network. However there are some other constraints the design that would not always allow the system maintain the discharge at optimum power transfer region.

In RF discharges, the electrons can only gain oscillatory energy from the oscillating fields. Without the collisions, the electron motion is coherent and no power can be absorbed from the RF fields once the particles have acquired their steady-state values of oscillatory motions. It is the only displacement current flowing out of phase with the applied field. The work done by the oscillating field is possible with the conduction current which resulted from the collisions.

2.2.2 Breakdown mechanism of the RF CCD

On both the RF and the DC cases, the basic determining factor for the breakdown threshold is the "*pd*" parameter. However the underlying mechanisms are quite different.

The DC breakdown is essentially depended on, “first Townsend coefficient”; the probability that electron will ionize a gas atom as it travels 1 cm along the discharge tube. This results in an amplification factor of “exp(α*d*)”. Electrons are released as the primary electron reaches the anode at distance “*d”*. This also implies that “exp(*αd*)” ions are produced by the primary electron. To preserve charge neutrality in steady state, these ions have to be given up at the cathode. On striking the cathode the ions produce secondary electrons with efficiency “γ” (the second Townsend coefficient)[16].

Thus electrons are released by the bombarding ions. In the previous pass, one electron leaving the cathode had eventually been lost by recombination at the anode. In order to compensate for the loss of this electron and to keep the discharge going, the ions bombarding the cathode must release at least one secondary electron a minimum with respect to *pd*, called the Paschen minimum. For the large values of *pd*, the number of collisions within the length of the tube is large.

proportional to υ_c. This also implies that, in a steady state, the absorbed energy goes primarily into heating the neutrals.

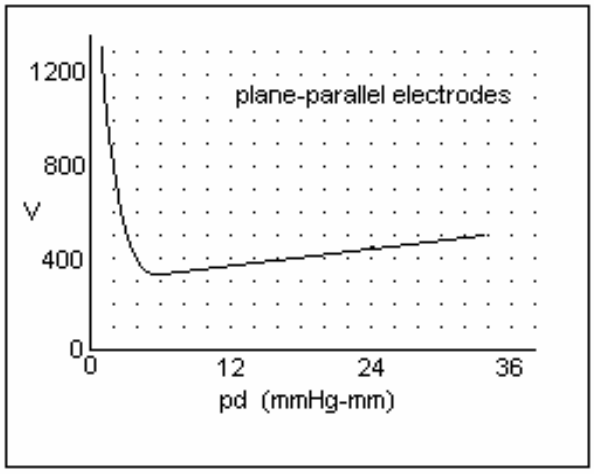

Fig 4. Breakdown Threshold vs. pd (air) [22]

Thus the electrons pick up very little energy between collisions so that the probability of ionization decreases. To compensate for this decrease, breakdown voltage rises. For small *pd*, breakdown voltage rises again because the collisions within the tube are too few. In the presence of a dc electric field, an electron can keep gaining energy continuously till it has sufficient energy to ionize a gas atom. Collisions therefore do not play any significant role in the ionization process in such discharges, except to retard the motion of the electrons.

Due to the nature of the RF discharges discussed on previous section, collisions play a significant role on the determination of the breakdown threshold of the discharge. Although the behavior is similar to DC case the reasoning is quite different. When an electron suffers a collision, its oscillatory motion is disturbed and its momentum randomized.

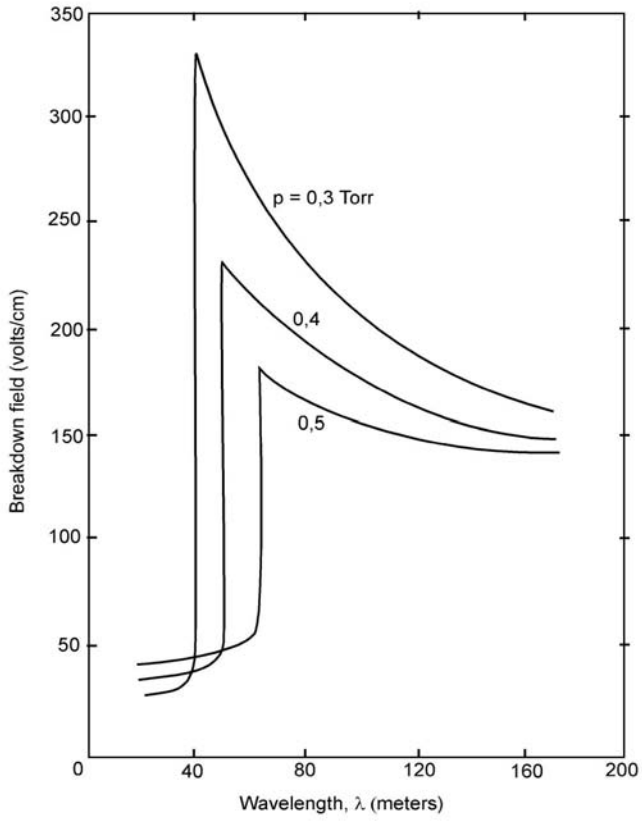

Fig 5. Breakdown field strength versus RF wavelength [23]

On the case of moderate pressures the collision frequency "υ_c" of the electrons are essentially greater than the field frequency "ω".

For the discussion restricted with the moderate pressures, the energy transferred to the neutral gas atoms in a collision equals the energy gained by the electrons in the time between two collisions. Thus, necessary field to accomplish breakdown increases with increasing υ_c, and hence with increasing pressure since *p* is As stated previously, while $\upsilon_c << \omega$, the collisions are few and far between, so that many cycles of the wave period go by before a collision occurs.

Thus at low pressures, the breakdown field strength increases with decreasing pressure, much like it does on DC fields. Since the breakdown field is raising both with the high- and low-pressure regimes, this implies that there must be a region in between where the breakdown field is a minimum. Again it turns out that this minimum occurs at a certain pressure where the equation satisfies $\omega \approx \upsilon_c$ condition at the minimum.

2.2.3 Space Charge Sheaths

The edge of the plasma in contact with the chamber wall, electrodes or some other surface is significantly different from the bulk plasma regions. A dark space or sheath is usually observed adjacent to all surfaces in contact with the plasma. The sheath is a region over which there is a significant voltage drop, and, as a result, there is an extremely low electron density. The electron density is very low because of the their high mobility relative to the slow ions. The electron thermal velocity is 100 times more than the ion thermal velocity [15]. These fast moving electrons will be absorbed rapidly if they reach the walls. Since the electron densities of the sheaths are quite low, the gas mixture there is excited only on low levels and remains dark.

A sheath region acts as an interface between the plasma and the electrodes. The force acting on the electrons will reflect the electrons moving from the plasma to the walls, back into the plasma. On the other hand ions from the plasma entering the sheaths will accelerate to the walls of the chamber. Although on each case the plasma

region have similar characteristics, space charge sheaths may have quite complicated specifications for the given conditions.

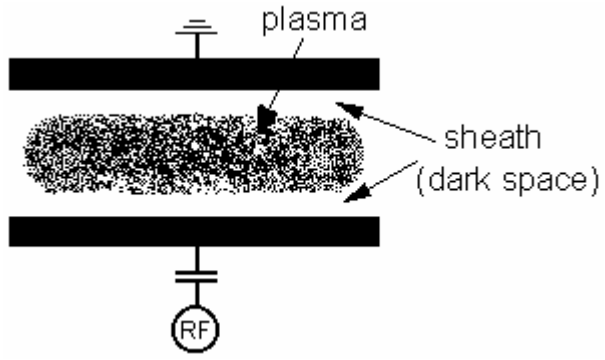

Fig 6. Space charge sheaths

Observing a given discharge, apart from the space sheaths, there may appear some other regions so called “negative glow” and “faraday dark spaces” [13]. Less bright regions of negative glow are due to the excitation of atoms by energetic electrons arriving from the sheath, accelerated from the strong field. The field neighboring the sheaths is not strong enough to give its energy to the electrons and is dark. This region with out the ionization and excitation processes is called the faraday dark space.

In the high frequency range where, the sheath is primarily capacitive, the sheaths that separate RF electrodes from the plasma usually dominate the electrical properties of discharges. Sheaths are poor conductors. There are some models proposed to explain the electrical properties of RF sheaths and to relate them to the dynamics of particles within the sheaths [16][17][18]. These models will be helpful on the following sections, in order to illuminate the effects of the RF shields to the properties of the active medium of a CO_2 laser.

Although the sheath thickness is dynamic, taking values from d_s=0 to $d_{s\ max}$ over a whole cycle of the field oscillation, sum of the thickness’ of two sheaths of a two electrode system will remain constant. An average for the sheath thickness

proposed by the authors of [13], by equating it to real displacement amplitude of the electrons,

$$\omega = \upsilon_c \Rightarrow \bar{d}_s \approx \frac{eV_a}{Lm\omega\upsilon_c} \tag{2.12}$$

$$\omega ? \upsilon_c \Rightarrow \bar{d}_s \approx \sqrt{\frac{V_a}{8\pi en}} \tag{2.13}$$

and it is also important to note that,

$$d_{s\max} = 2\bar{d}_s \tag{2.14}$$

2.2.4 RF CCD Modes

At moderate pressures, under exactly same conditions such as of the gas composition, gap geometry, field frequency and electron voltage, RF discharges have two basic different types of distinguishable properties. First observations are made by S.M. Levitsky in 1957. Levitsky termed these two types of discharges as an α-discharge (low current discharge) and a γ- discharge (high current discharge). The α and γ modes essentially differ in the distribution of basic characteristics that influence the laser effects, the plasma density, the RF field amplitude, intensity and luminosity. Besides, of the great importance they effect ionization in the electrode sheaths and current closure mechanisms on the electrodes [13]. However, α- and γ-modes at low pressures, they do no more have distinguishable properties of the great importance.

2.2.4.1 α-Discharge

For a given laser cavity at moderate temperatures, until the breakdown point is reached and the discharge is initiated, the current and the voltage is proportional indicating the active medium behaves like a capacitor, reactive current is flowing trough the system.

At moderate pressures the α-discharge exhibits the effect of normal current density, at about 1-10 mA cm^{-2} as it is on DC discharges [13]. While at low pressures

it does not. At moderate pressures the α-discharge does not occupy all the area of a large electrode. After the discharge is initiated, if the current is further increased on controlled amounts, the glow that has appeared on the center of the electrodes until the it covers all the electrode area. If two electrodes differ in area, it does not affect the size of the current spots on each of the electrodes and the voltage will remain the same. Until the entire electrode area is covered with glow discharge, then the voltage will also begin to respond the further raised current proportionally. The gap in

Fig 7. Typical α- discharge

between two electrodes is formed of two sheaths neighboring the electrodes are followed by bright areas of discharge and the area at the center of the gap is less bright.

The sheaths on α-discharges are relatively thick. In fact they might be considered gas gap containing no electrodes with variable thickness which two times over a cycle being with the maximum and zero thickness

Their thickness is decreased with the increasing frequency of the applied field. Equation (2.11) is further approximated for the α-discharge at moderate pressures by the same authors [13] to give a better understanding of the mean sheath thickness,

$$d_{s\alpha} \approx \frac{v_d}{\omega} \tag{2.15}$$

Also at moderate pressures the α-sheath ion density is of the order of the plasma density. There is only a partial ionic current flowing. Since the sheaths are not good conductors, electrodes do not have conduction current on them whether they are covered with dielectrics or not. The conduction current is limited inside the plasma.

The α-discharge is operative within a limited, current density, which is not large in variation. Again it is not operative in any gap and pressure combinations. If the product *pd* is higher than a critical "pd_{cr}" value for a given gas or gas combination the α-discharge will be unstable or impossible. The critical *pd* value for molecular gases is essentially lower than the atomic gases. It will be difficult to obtain α-discharge with rough current adjustments or rather small electrode areas. The limiting values of the α-mode increase with the frequency.

2.2.4.2 γ- Discharge

Followed by the further increase on the normal current density, after a critical point is reached, the discharge changes its appearance. A contraction in the discharge occurs. Across the electrodes current density is increased and again voltage drops. Trough the cross-section of the plasma, new sheaths, faraday dark spaces, bright negative glows and the brightest positive column at the center is observed.

Immediately after the threshold value for the current density inside active medium is achieved, a breakdown in the sheaths in the same sense of the DC breakdown in the Paschen curve occurs. Oscillating electrons will satisfy the Townsend criteria and secondary electrons are emitted. That is why the γ- discharge is has a lot in common with a DC glow discharge. Through the one single cycle of the alternating electric field, the discharge behaves like DC glow discharge. When the electrons reach the electrode they produce electron emission and the produced electrons are multiplied in the sheaths. A sheath of the γ- discharge also resembles the cathode sheath of a DC discharge. The normal cathode fall voltage is independent of the pressure ant the sheath thickness is inversely proportional to the pressure. The relationship (2.15) is also valid for the sheath thickness of the γ- discharge. It is relatively thin compared to the sheath thickness of an α-discharge. The thin γ-discharge sheaths possesses better conductivity and are able to pass the displacement current in the case of a strong electric field. Charge multiplication is maintained in the sheaths, gas is highly ionized to a greater charge density. This leads to strong

conduction and displacement currents in the plasma. At relatively high pressures of about *p=50 Torr*, both current components become comparable [13].

Trough the cross section of a γ- discharge, sheath region is followed by rather bright section of negative flow. The negative glow is due to the excitation of atoms by accelerated energetic electrons arriving from the adjacent sheath. The negative glow section is followed by the faraday dark space. The faraday dark spaces are due to the electrons lacking of energy and the drift is slow. Trough this region the field is not effective and excitation and emission cease. However since the ionization rate is so low, the drift current replaces diffusion current and the field again recovers. The field again compensates the electron energies and if the gap is enough thick, faraday dark space is transformed in to the positive column.

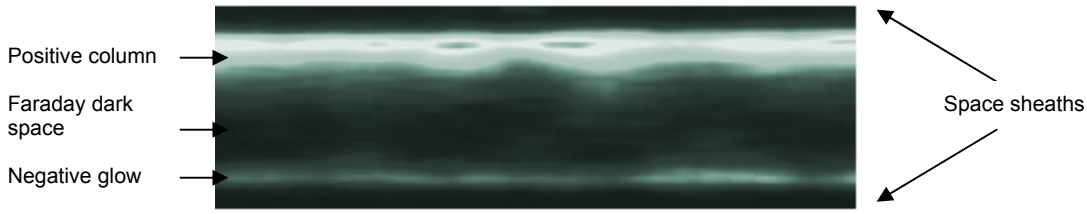

Fig 8. The γ- discharge

2.2.4.3 α- γ Transition and Their Co-Existence

In the range of moderate pressures α- γ transition occurs suddenly and changes all the structure of the plasma. The electrode current density and current to voltage proportionality change suddenly. After the electrodes completely covered by plasma spot, the α-mode becomes anomalous, and the electrode voltage grows with discharge. The voltage amplitude in the sheaths also rises because as the discharge current density gets higher, and so that the ion density. After the average voltage on this average thickness of the gas gap approximately reaches the breakdown point on the "Paschen curve" of the corresponding gas mixture the transition occurs in other words the critical ion density is achieved.

This critical plasma density is proportional to the period of the applied field. This relationship is due to the increasing the frequency the stealth thickness is

reduced and with the reduction of the sheath thickness the ion density is increased. For the sheath voltage fall to reach the breakdown voltage value and the transition occur, the ion density in the plasma sheath must be larger.

Transition voltage increases with increasing pressure and decreasing frequency. Transition current slightly reduces as the pressure grows and strongly rises with frequency.

In the α- γ transition region there are some hysteresis effects. As the current and voltage are increased, the α-mode transforms to the γ-mode with a current strength corresponding to a constant power, which does not change at transition. If the γ- discharge current is reduced, the back transition is delayed and occurs at a lower current and power than those achieved in the γ-discharge as a result of direct α- γ transition.

The both α- and γ-modes may be observed inside the active medium simultaneously, when the operating voltage of the normal α-mode is lower than of the normal of the γ-mode. If the gap current is increased gradually starting from lower values, there is no discharge at first and only capacitive reactive current is flowing. Then at a sufficiently high voltage, a breakdown occurs and the voltage will fall to normal operating voltage of the α-discharge.

As described previously if the current is further raised, the spot gets larger and covers all the electrode area and the α-discharge becomes abnormal. Followed by the increase on the voltage the breakdown value is achieved and the γ- discharge is initiated. The discharge than is immediately contracts to a rather thin filament while the electrode voltage drops to normal γ- discharge voltage. This voltage is valid for the whole area including the current free periphery. Since this voltage here on the current free periphery is higher than the ignition voltage of the α-discharges, depending on the current characteristics one may occur.

The heating and the thermal expansion of the gas due to the heat release from the γ- discharge filament and possibly the gas ionization from the filament radiation stimulate breakdown and ignition of α-discharge in this current free area. This occasionally occurs with sub-normal modes of the γ- discharge, when threshold

current density for α-discharge fall bellow the threshold current for α- to γ- transition for some discharge circumstances.

2.2.5 Current Voltage Characteristics of CCD

Apart from experimental results, one can make use of theoretical models for RF CCD and "particle in cell (PIC)" simulations, to have a better understanding of the current-voltage behavior in the active medium of a given CO_2 laser. With the help of this information gathered from this numerical information, expectations from the proposed device will be clearer.

2.2.5.1 The Conduction and Displacement Current

Current density resolved from the canonical forms of the Maxwell equations;

$$\nabla \times \mathbf{B} = \mu_0 \mathbf{j} + \mu_0 \varepsilon_0 \frac{\partial \mathbf{E}}{\partial t} \tag{2.16}$$

$$\nabla \cdot \mathbf{E} = \frac{1}{\varepsilon_0} \rho \tag{2.17}$$

with the assumption that no magnetic field is involved due to the specifications of the application, appears to have three basic components. There exists the "displacement current",

$$j_{dis} = \frac{1}{4\pi} \frac{\partial \mathbf{E}}{\partial t} \tag{2.18}$$

The displacement current has no association with the existence or the motion of the free charges. Secondly there exists the "polarization current",

$$j_{pol} = \frac{\partial \mathbf{P}}{\partial t} \tag{2.19}$$

Polarization current is due to the polarization of the atoms and ions. It has relatively small strength and can be neglected. Finally there exists the "conduction current" associated with the free charge motion and obeys the Ohm's law.

$$j_{cond} = \sigma E \tag{2.20}$$

In the range of high frequencies of this thesis concern, the values for the current density $j = \sigma E$ and the dipole moment $P = \chi E$ for the steady states are no more valid. The current density and the dipole moment is not only depends on the oscillating field but also to the history of the field. However exploiting the super position principle some important current related specifications of the plasma could be derived from the current equation which can be produced from the Maxwell equations (2.19) and (2.20),

$$\mathbf{j} = \left(\sigma + i \frac{\omega(\varepsilon - 1)}{4\pi} \right) E \tag{2.21}$$

where the field is expressed as,

$$E = E_0 e^{i\omega t} \tag{2.22}$$

rather than (2.6). Imaginary components of the current density may be out of phase and many of the constants involved may depend on the frequency of the oscillating field. The displacement current is not involved on the energy dissipation in the active medium. However equation (2.21) has the form of the Ohm's law and we can express the complex conductivity or complex permittivity of the medium with respect to the current density. Utilized the microscopic analysis of the electron motion in the plasma from equation (2.1) gives out the dielectric permittivity and the conductivity of the plasma [13];

$$\sigma = \frac{e^2 n_e \upsilon_c}{m\left(\omega^2 + \upsilon_c^2\right)} \tag{2.23}$$

$$\varepsilon = 1 - \frac{4\pi e^2 n_e}{m\left(\omega^2 + \upsilon_c^2\right)} \tag{2.24}$$

An approximation of $\omega^2 = \upsilon_c^2$ is valid for moderate pressures so figure for the conductivity reduced to

$$\sigma = \frac{e^2 n_e}{m \upsilon_c} \tag{2.25}$$

Another important specification for a given is charge event is the electron mobility,

$$\mu_e = \frac{e}{m \upsilon_c} \tag{2.26}$$

and conductivity can also be expressed with electron mobility for clearer expression,

$$\sigma = e\mu_e n_e \tag{2.27}$$

The density of discharge current that flows on the over all circuit is also flowing trough the plasma. Although the electrodes can be assumed as ideal conductors and has no displacement current component, among the active medium conduction is poor and there is a field a field attached. This field generated on the plasma has the strength,

$$E_p = 4\pi\left(q + end_s\right) \tag{2.28}$$

where "d_s" is the sheath thickness and "n" is the plasma density.

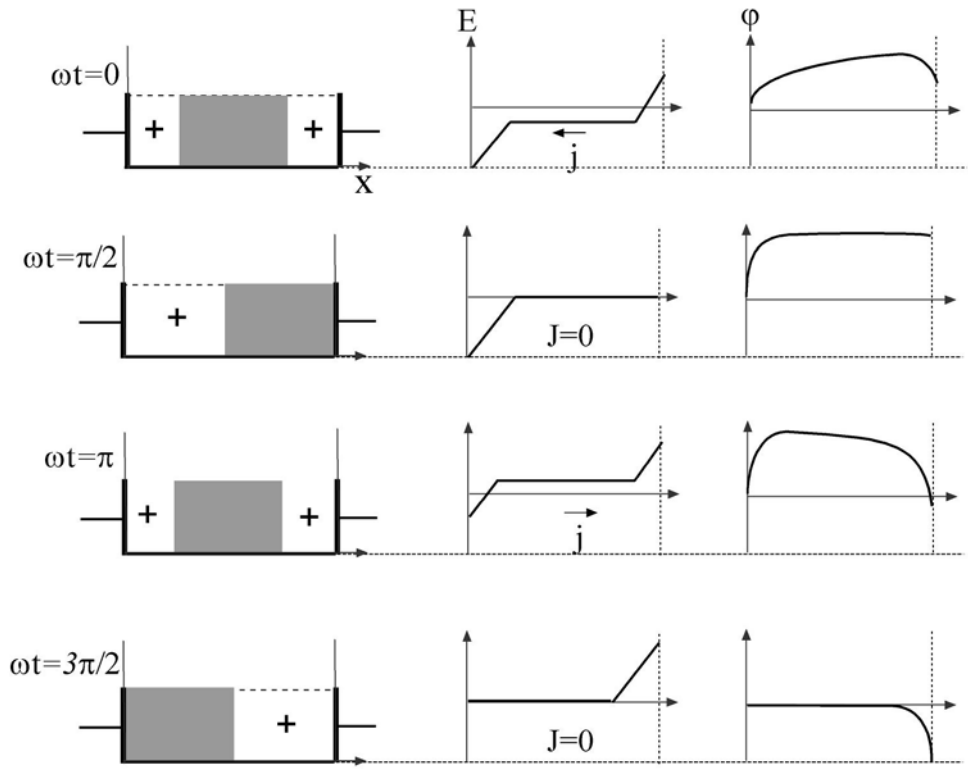

Fig 9. Single cycle of the oscillating field

Simply the discharge current is the flowing charges per unit time,

$$j = \frac{\partial q}{\partial t} = -en\frac{\partial x}{\partial t} + \frac{\partial E_p}{4\pi} \tag{2.29}$$

and the plasma specific field of (2.28) could be substituted,

$$j = -en\frac{\partial x}{\partial t}\left(1 - 2A/L\right) + i\omega V/4\pi L \tag{2.30}$$

Clearly when $n=0$, that is while there is no discharge, the first term is absent and there is only the reactive current of a vacuum capacitor formed in between the electrodes with the capacitance per unit area of the electrodes,

$$C = 1/4\pi L \tag{2.31}$$

2.2.5.2 The Potential Among the Active Medium

The time average harmonic potential of the electrodes is zero whilst the plasma potential is always positive with respect to the electrodes. This can be explained with the same approach that is used with the discussion of the breakdown criteria.

When a finite-sized plasma is formed, the electrons being the more mobile species, tend to escape from the plasma much more rapidly than the ions. The plasma is therefore left with an excess of ions, which makes it slightly positively charged with respect to its original neutral state.

With respect to the electrodes the plasma acquires a definite potential “the space potential”. This potential depends on the geometry and extent of contact with the different electrodes, the potentials on these electrodes and the amount of excess positive charge left behind with the plasma by the escaped electrons. The potential adjusts itself so that it is more positive than the most positive electrode. Near the electrodes however, the plasma potential has to change sharply to conform to the potentials on the electrode surfaces. This is achieved by the potential changing across a sheath region that acts as an interface between the plasma and the electrode.

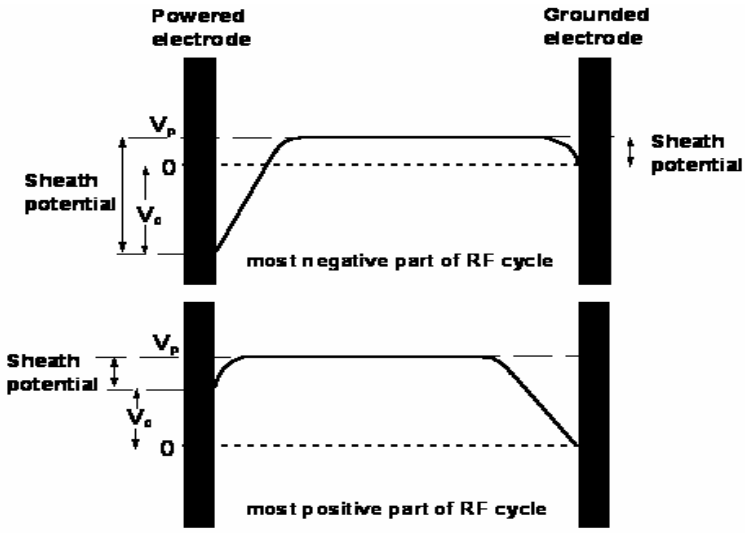

Fig 10. Sheath Potentials

Instantaneous voltage fall on a sheath relative to the corresponding electrode from the discontinuity of the field [13];

$$V_s = 2\pi end^2 \tag{2.32}$$

An expression for the mean value of the constant plasma potential may be evaluated exploiting the fact that it should be in balance with the mean value of the voltage fall on the sheaths. The approximated value for d_s at moderate pressures was given (2.12), also substituting this, the mean voltage fall on the plasma made clear further.

$$\bar{V}_p = \frac{3\pi en\mu_e^2 V_a^2}{L\omega^2} \tag{2.33}$$

Positive plasma potential is a very important feature of the RF discharges, especially on deposition and etching applications.

The voltage to be applied to the electrodes is determined from the necessity of having a normal current density through the plasma. The applied voltage should be the sum of the voltages on the sheaths and positive column of the plasma. This sum is a function of the current density and will have a definite minimum on the

current-voltage characteristics of the active medium. This minimum is important to satisfy the normal operating conditions.

The electrode voltage should be the sum of the voltages on the sheaths and positive column of the plasma. Potential on the positive column is left rather indefinite. Nevertheless authors of [13], exploiting the fact that field to pressure ratio for a given system should approximately fixed, they made an assumption for the positive column voltage to be in the form of,

$$V_{pc} = CpLj^{-m} \tag{2.34}$$

where C and $m>0$ to be constants. Also assuming a half cycle phase difference in between the positive column voltage and the sheath voltage the applied voltage is determined as follows,

$$V = \sqrt{V_s^2 + V_p^2} = \sqrt{\left(\frac{4\pi dj}{\omega}\right)^2 + \left(CpL\right)^2 j^{-2m}} \tag{2.35}$$

$V\left(j\right)$ function has a minimum for,

$$j = \left(\frac{\omega CpL\sqrt{m}}{4\pi d}\right)^{1/(m+1)} \tag{2.36}$$

representing the normal current density for the α-discharge. Obviously the minimum condition for the normal current density will be raised with increased field frequencies, indicating that it is possible to achieve higher current densities with out disturbing the normal current regime with higher frequencies.

In the same sense an expression for the normal current density of the γ-discharge is evaluated. Since the displacement and the conduction current are $\pi/2$ out of phase,

$$j = \sqrt{j_n^2 + j_{dis}^2} = C_1 p^2 \sqrt{1 + \left(\frac{\omega V}{4\pi C_1 C_2 p}\right)^2} \tag{2.37}$$

The constant C_1 has the origins from the conduction specifications of a DC glow discharge and related to the properties of the gas mixture and electrode material. The constant C_2 is directly related to the pd value of the medium.

2.2.5.3 Impedance of the Active Medium

With the oscillating field applied but without the initiation of the discharge, any simple active medium arrangement with its two electrodes behaves like a vacuum capacitor. The reactive current is flowing trough and on the load side the system has a certain capacitive reactance.

Followed by the ignition of the discharge in the active medium, considerable increase in capacitance and active conductivity of the gap after plasma is produced. Before the initiation of the discharge, the gap capacitance was determined by the distance between the actual electrodes, after the initiation of the discharge it is determined by the total sheath thickness. On the discharge circumstances, the distance between the electrodes is reduced, a plasma conductor is introduced in the gap middle with resistive and capacitive components, and also there exists two large variable series capacitance of the sheaths. Their equivalent capacitance is approximately constant in time and about the maximum thickness of one of the sheaths.

Since the equivalent network components of the active medium possess sheaths of the two electrodes as capacitors, calculation of the impedance of these capacitors may be convenient for estimating the impedance behavior on dynamic conditions. For the high-pressure, collisional Lieberman model [18] the capacitive impedance of the sheath, *Zs,* can be expressed as;

$$Z_s = 0.803\left(\frac{e}{\omega^5 \varepsilon_0^3 A^3 m_i}\right)^{1/5} V_s^{3/5} j_{o+}^{-2/5} \lambda_i^{1/5} \tag{2.38}$$

where A is the electrode area, m_i is the ion mass, λ_i is the ion diffusivity mean free path, V_s is the amplitude of the fundamental component of the sheath voltage. j_+ is the DC ion current. It is amplitude defined to be,

$$j_{o+} = en_+ v_+ A \tag{2.39}$$

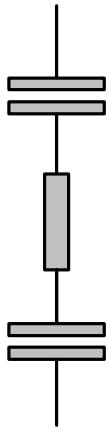

Fig 11. Active medium equivalent circuit

Together with the conductivity and permittivity discussed on the previous section; the impedance of the load can be expressed as the series network of two capacitors and a resistor combination. Another approach to the plasma impedance is the Godyak-Stenberg model is exploited this assumption. Impedance of the active medium can be interpreted as being the complex resistance of the Ohm's law. Implementation of the previously defined values for the current density and the voltage applied to the electrodes, the impedance is calculated to be [13];

$$Z = \frac{V}{j} = \frac{\dfrac{Lm\left(\upsilon_c + i\omega\right)}{e^2 n} + \dfrac{8\pi d}{i\omega}}{\dfrac{1-\omega^2}{\omega_p^2} - \dfrac{i\omega\upsilon_c}{\omega_p^2}} \tag{2.40}$$

Here "ω_p" is the plasma frequency and plains the equation (2.24) to give,

$$\varepsilon = 1 - \frac{\omega_p^2}{\omega^2 + \upsilon_c^2} \tag{2.41}$$

At moderate pressures plasma frequency can also be approximated to remove the divisor.

$$\omega_p = \sqrt{\frac{4\pi e^2 n_e}{m}} \tag{2.42}$$

Although the system is non-linear with the sheath thickness and the electron density is depended on the voltage amplitude again, assuming that there exists a strong ionization, that is $\omega_p^2 \; ? \; \omega^2$ and $\omega_p^2 \; ? \; \omega\upsilon_c$, the equation can be expressed in a more definite way [13],

$$Z = \frac{L}{\sigma_t} + \frac{8\pi A}{i\omega} \tag{2.43}$$

where σ_t is the complex plasma conductivity. Complex conductivity of the medium in case of free charges is the result of the retardation effects of the rapidly oscillating field. Its amplitude is given with the relation,

$$\sigma_t = \sigma + i\omega\frac{\varepsilon - 1}{4\pi} \tag{2.44}$$

with the values of the conductivity and the permittivity of the medium given with equations (2.23) and (2.24). Substituting complex conductivity of the plasma becomes,

$$\sigma_t = \frac{e^2 n}{m\left(\upsilon_c + i\omega\right)} \tag{2.45}$$

The latter model improved by V.A.Godyak and N. Stenberg [19] compared to the former one by M.A.Lieberman is claimed to be more consistent with the experimental results [20].

2.2.6 The Electrodes

Unlike the DC discharges, RF discharges can operate on both α- and γ-modes regardless of whether the electrodes are in contact with the plasma or separated by a dielectric in between. None of the plasma characteristics will be disturbed but the electrode voltage. Also some other specific effects may be expected on the voltage dependent values. Besides it is possible to take the some important advantages of these influences.

The electric equivalent of the load of the system was composed of two capacitors and a series resistor, as it was discussed previously. The sum of the

capacitance per unit area was given with relation (2.30). For the dielectric material to be coated with thickness "δ" and the dielectric permittivity of "ε", the total capacitance per unit area is changed to become,

$$C = \frac{1}{4\pi\left(d + \frac{2\delta}{\varepsilon}\right)} \tag{2.46}$$

and this new expression for the capacitance will have its influence on the electrode voltage of an α-discharge as,

$$V = \sqrt{\left(\frac{4\pi\left(d + 2\delta/\varepsilon\right)j}{\omega}\right)^2 + \left(CpL\right)^2 j^{-2m}} \tag{2.47}$$

with the modification of "*L*" is now is the distance between the dielectric coatings.

In the same sense the minimum condition for the current dependent function of the electrode voltage on a proper α-discharge is re-expressed to be,

$$j = \left(\frac{\omega CpL\sqrt{m}}{4\pi\left(d + \frac{2\delta}{\varepsilon}\right)}\right)^{1/(m+1)} \tag{2.48}$$

It can be summarized that the new value for the normal current density will be lower for its corresponding minimum electrode voltage while this voltage will settle on a higher value.

The first one of the two practically important conclusions is that coating the electrodes with materials possessing poor emission properties can increase the breakdown sheath voltages without affecting the discharge properties. The voltage fall and the sudden decrease on the load impedance after the breakdown will be less severe.

Secondly, the least possible normal current density for the α-discharge is decreased while the threshold value before a transition occurs is remained the same. As will be discussed among the next section; on most of the circumstances an α-discharge is more favorable for achieving a proper population inversion inside the cavity. Now the current density range for the normal operation of α-discharge is

broader and the applied power and so that the obtainable optical laser power can be raised to a higher value with out the risk of transition to an unfavorable mode.

In the same sense the minimum current density for the proper operation of the γ- discharge is also lower now. Dielectric coating of the electrodes permits subnormal states of the γ- discharge, which may be useful for the designer on many circumstances.

When the electrodes are completely covered with the electric, it stabilizes the discharge provided by the strong negative feedback between the dielectric and the discharge. Here the dielectric serves as distributed reactive ballast over the surface of the electrodes. Stabilization effect is more effective when the dielectric thickness to dielectric permittivity ratio is higher than the sheath thickness, which is more likely to happen with γ- discharge.

However there is an even more interesting consequence of the discussion is that, as mentioned previously, critical current density for γ- discharge is being lower than of the threshold current density for α- γ transitions. On the same range of current densities co-existence of the α- and γ- modes may become permissible.

It may also be useful to note that in the absence of any reference electrodes in contact with the plasma, the plasma potential becomes undefined.

Such insulation material usually impairs the heat removal and plasma density will become lower or gas mixture may suffer further disassociation. Nevertheless this is usually the concern of the higher end of range of the current densities of the γ-discharge.

2.2.7 Dependencies of Discharge Parameters on the Field Frequency

Discussions among the previous chapter have stated that all the variables of the discharge properties are related to ω the angular frequency. The frequency dependence of the conductivity σ, electron density n_e, and the plasma field E_p are direct concerns of the proposed device, determining its specifications. It will be helpful to summarize the frequency dependencies of these properties of the

discharge. Besides it will also be very helpful to exhibit these dependencies with convenient approximations making them clearer.

Probably while designing a CO_2 laser, the most important effect of the field frequency on the system among others is the thickness of the space sheaths of the α-discharge. As it will be stated on the following section α- type of RF CCD is the most convenient type of excitation over all for a large variety of CO_2 lasers. The space sheaths are the inseparable components of the α-discharges.

System can only operate in α-mode on a certain frequency range that depends on the size of the gap *L*. The upper and lower frequencies are limited. For an α-discharge to be ignited easily in the gap it is necessary that size of the gap should be larger than the maximum sheath thickness which is inversely proportional to the field frequency. In order to have enough space for the plasma serves as the active laser medium, *L* must be quite large compared to the sheath thickness. Since better heat removal conditions or waveguide designs require smaller *L*, this improves the rigorous restrictions on the lower working frequency the RF field. The direct relation of the sheath thickness with frequency is expressed with the relation (2.15).

Regarding the frequency dependency of the sheath thickness authors of reference [13] have also explored the frequency dependencies of the conductivity, electron density and current density.

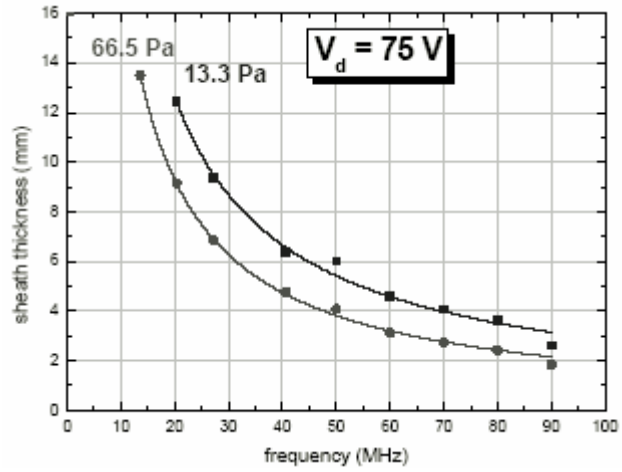

Fig 12. Sheath thickness vs. frequency [25]

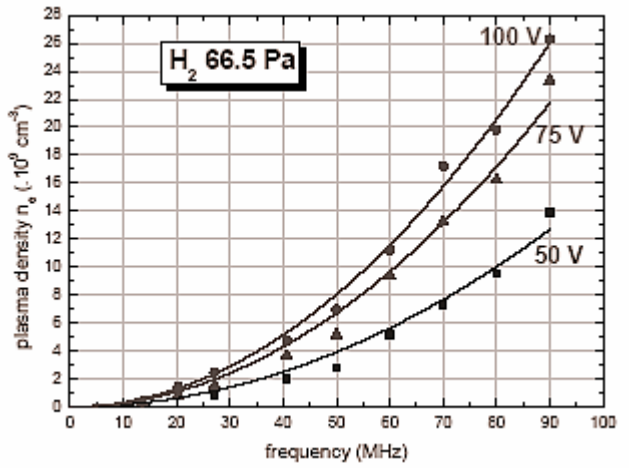

Fig 13. Plasma density vs. frequency [25]

They conclude a weak dependence at about $j_n : \sigma : n_e : \omega^{4/3}$, and proven this relation to be valid for the α-discharge at moderate pressures with experiments. Another important conclusion from these explorations is that the upper limits of current density "$j_{n\alpha\ tre}$" and the plasma density "n_{tre}" before α- to γ- transition are increased with the increasing field frequency. This may allow a raise of the obtainable optical power up to another limit resulted from heat removal considerations.

On the lower edge of the permissible frequency range normal current density and the energy output will be too small for proper generation of optical power. Similarly the higher RF frequencies are also unacceptable in order to avoid overheating of the plasma and not to exceed T_{max} limit of 600K. Exceptional situation is with the microwaves where λ is comparable to the gap size.

High frequencies may be disadvantageous if the quarter wavelength of the field oscillations is comparable to the electrode length, effect of wave retardation occurs making the discharge non-uniform. Although this may be solved with some special techniques, usually system tends to be more complex. Matching problems are also another technical difficulty arises with higher frequencies.

With the higher frequencies stray inductance and capacitance of the electrical network is increased. This leads to the more non-linear functioning of the system and loss of efficiency.

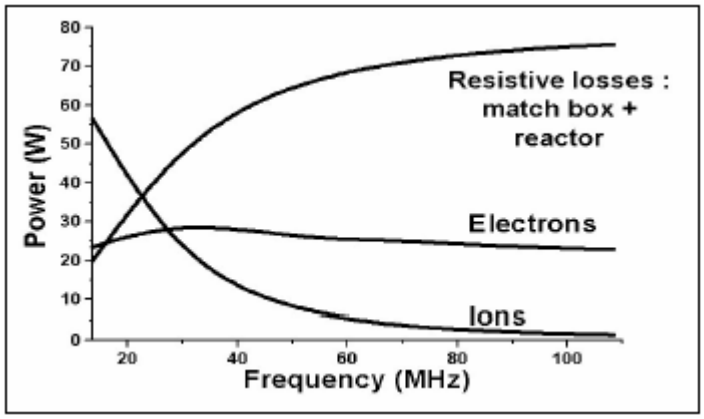

Fig 14. Model calculation showing where the power is dissipated when frequency varies [24].

2.3 Discussions in Favor of α-mode RF CCD for Active Medium

As far as some application specific circumstances are not accounted RF CCD as an excitation method seems to be disadvantageous compared to the DC excitation. Most of these disadvantages are due to technical problems such as that RF excitation is rather complex with the high cost of components and overall construction, difficulties of matching the RF generator to the discharge load, necessity to protect the personnel from harmful RF field by screening the whole setup and other special requirements of RF engineering. All the RF equipment will tend to behave non-linear especially because of their stray capacitance and inductance. Similarly all these components will tend to generate oscillations of the non-useful type. Compared to

RF excitation, clearly DC excitation is cost effective and more efficient with power and ease of usage.

However some CO_2 laser classes such as, the slab, the annular and the waveguide are only possible with RF excitation. These classes of lasers are of the great importance since they represent better solutions to the contemporary demands, most of which were represented on introductory discussions. The important point to be stated is RF excitation permits a variety of complex geometry that would be asked by the designer and many of which would not be possible with DC excitation.

Such designs may be free of fragile components, and will have all-metal constructions supported with dielectric insulators and coatings. These varieties of active medium may also benefit from the shorter distances for gas flow, thus rapid replacement of the laser gas.

Another outcome of these CO_2 laser designs with RF excitation is that with shorter gaps, they could be ignited at very much lower voltages compared to that of the DC excitations. Moreover the sudden voltage fall followed by ignition will not be severe any more.

RF excitation supports better modulation of the laser with less effort. The DC excitation requires large ballast to stabilize the discharge during modulation whereas for the RF case the power can simply be switched or adjusted.

The possibility of coating electrodes with dielectrics or placing them outside the chamber is an important outcome of RF excitation. Electrodes will no more be subject to plasma environment. The risk of electric shocks and short circuits will be reduced. The dielectric coatings on convenient circumstances may serve as ballast resistors of the DC case with out loss of efficiency. Likewise RF discharges can utilize reactive components as ballast resistors efficiently. The dielectric coatings may also serve optical purposes as it is in the case of waveguide CO_2 lasers.

RF discharges to create a suitable active medium for CO_2 lasers should be in the α-mode. The high current characteristics of a γ- discharge may overheat the plasma. Besides the discharge region through a γ- discharge contains strong ionic current, negative glows and faraday dark spaces which would lead to inefficient

usage of the active volume with most of the power being dissipated on heating of the plasma.

On the other hand an α-discharge will utilize most of the active volume including the peripheral regions and will be efficient on supplying desired collisions. However there are some possible CO_2 laser designs, utilizing the combined discharge of the α- and γ-modes or α-discharge together with a DC discharge especially of the fast flow types.

CHAPTER 3

PROPOSED EXCITATION SYSTEM FOR RF CCD CO_2 LASERS

The proposed system, the objective of this thesis work, will accept any one of the either three or mono phase mains power, in any voltage in between 80 and 250 Volts of RMS to convert it in to the convenient type of RF power to satisfy the demands of a CO_2 laser system described in chapter 2, without introducing any "cosφ" reactance and electromagnetic interference "EMI" back to the mains. Such a system is composed of four basic building blocks; the power factor corrector, the power supply, the RF generator and finally the impedance matching network.

As it was stated in the introduction chapter, proposed "all solid state" device should be as simple as possible with the least possible amount of components. This idea will be the policy to satisfy all other demands of the industry, such as being cost efficient both for investment and maintenance issues, reliability, durability etc.

3.1 The Proposed System

In order to achieve the goals discussed previously and to satisfy the demands of an active medium of a CO_2 laser, as discussed on previous chapter such a system is intended; The system will be composed of a general power conditioning unit including a DC rectifier, a power correction unit "PFC", a switch mode power supply "SMPS" will deliver the necessary power at 250 Volts to a Class-E RF power

generator in combination with an impedance matching network capable of adopting it self to ignition and plasma maintenance conditions. A phase locked loop “PLL” frequency synthesizer will determine the frequency of the applied field. Whole system will be solved with an all solid-state design.

Class-E amplifiers consist of a single active component with their basic design. The output power of each amplifier is limited with the capabilities of this active device. Although active devices can be used in parallel or series combinations, such solutions require additional efforts to balance the power and further tuning problems.

Large areas of electrodes for RF discharges are known to cause instabilities and disturbed distribution of the discharge trough the active medium. Various efforts have paid to overcome such instabilities, e.g. [24]. However due to the nature of the application of this thesis interests, larger electrodes are not necessary trough the active medium. Having the electrodes divided into pieces through the longitudinal distance of the active medium will perfectly solve the problem.

Followed by the latter two reasoning, the system is resolved from a series of class-E amplifier modulus each combined with its own impedance matching network. Each of this amplifier units will draw “2.88 A” of current at “250 V”, to supply a RF power of 720W delivered to the self-matching network. The designer will be free to make decisions about, how many electrodes should be fed by each module according to the size and power requirements of each electrode or likewise how many such modules will be used for the whole active medium.

Each module will be fed for power from a single power-conditioning device, which will also be operating with the supervisory system control. Amplifier modules would not contain control circuitry or would not need to accept control signals. Rather every module will be initiated or finalized operation or perform modulation directly by the control of the applied power. They only will consist output terminals connected to the supervisory circuit sending error signals or some useful information about operational conditions, such as the standing wave ratio “SWR”.

The power conditioning system can be designed with either one of the two alternatives, selects due the amount of the necessary power or the circumstances about the mains. The first one of these two alternatives, a buck converter fed with

DC from the rectifier followed with a boost converter serving as PFC to supply adjustable 280 V. This solution is easier to construct and cost efficient. However it is not as reliable as the second alternative where the PFC circuit fed from the DC rectifier is followed by a half or full bridge SMPS to supply adjustable power of the desired quality.

The former alternative can also be constructed on a single board with the amplifier module and the supervisor circuitry, in order to obtain a complete module RF plasma generator.

Of the usual practice, CO_2 lasers exploit self-excited power generators made from electron tubes "valves" in the laboratory environments and class-C mode amplifiers on commercially available products made both with valves or solid state active devices. These types of systems, when a large amount of power is necessary, require powerful cooling and large spaces. They lack of efficiency and increase maintenance costs. They may contain fragile components and heavy transformers.

The class-E solution, major issue of this thesis work, is believed to differ from these previous designs with a substantial performance on efficiency and with the volume occupied. This restriction on the size of the transistor can limit the performance of class-E amplifiers.

RF generator implementation of class-E systems for RF plasma and RF heating applications are previously discussed by various authors and stated to be feasible, successful and promising [29][30][33][36][39][41][43][44]. These papers investigated class-E operation at 13.56 MHz. 13.56 MHz is one of the Industrial, Scientific, and Medical (ISM) frequencies and probably one of the most convenient one for CO_2 laser applications due to the discussions of chapter 2 and capabilities of commercially available cost efficient active devices. This frequency will introduce less problems of the high frequency behavior compared to higher ranges of ISM frequencies.

As the term refers, ISM frequencies are defined on allocation tables of international and national standards and regulations, to be used with for a wide variety of applications such as plasma generation, RF heating, and semiconductor

processing and likewise applications of industry, medicine and science. Higher harmonic levels of the frequency 13.56 MHz are also defined to be ISM frequencies.

Since 1992, industrial 13.56-MHz RF power generators, using class-E output stages have been manufactured by Dressler Hochfrequenztechnik (Stolberg, Germany) and Advanced Energy Industries (Ft. Collins, CO). They typically use RF-power MOSFETs with 500- to 900-V breakdown voltages made by Directed Energy or Advanced Power Technology and produce output powers of 500 W to 3 kW with drain efficiencies of about 90 percent.

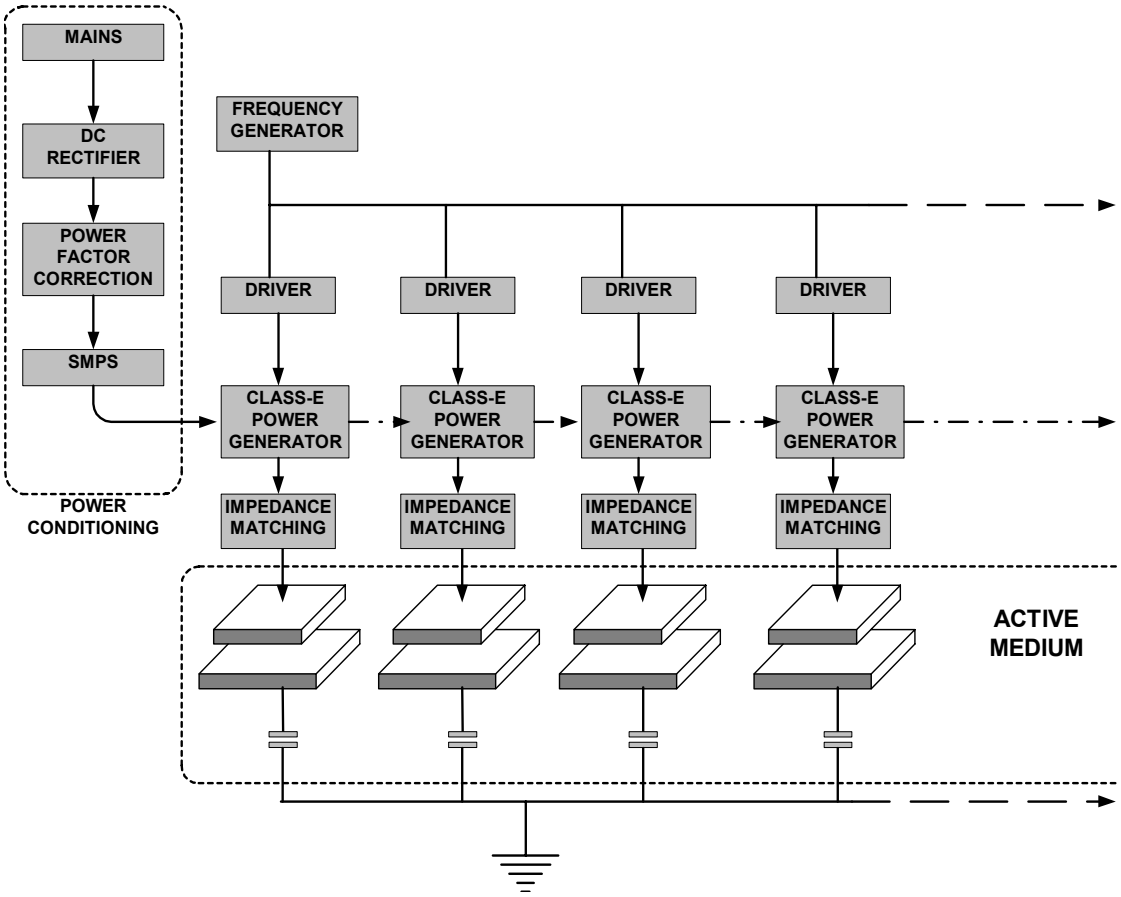

Fig 15. Implementation of Proposed System on Multiple Electrodes

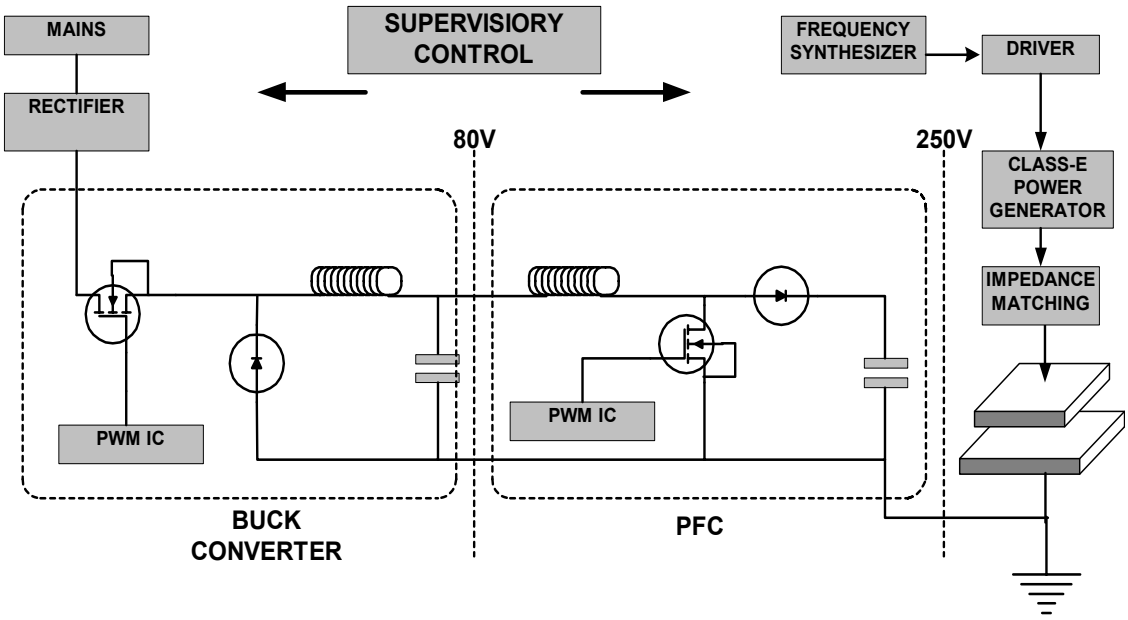

Fig 16. Implementation of Power Conditioning on Complete RF Generato r

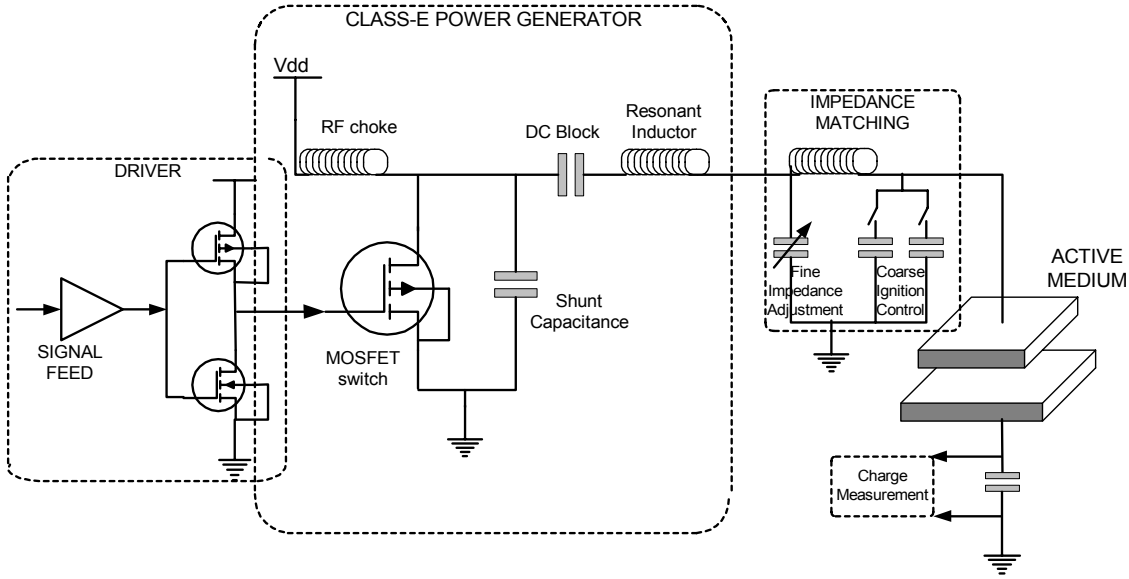

Fig 17. Impedance Matching Combined Class-E RF Generator

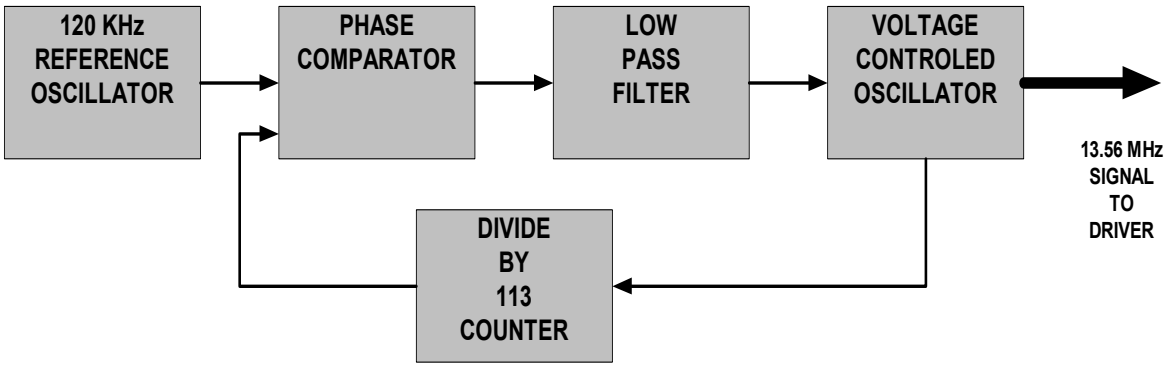

Fig 18. The Frequency Synthesizer

3.2 The RF Power Generator

The RF power generator to be used for the proposed system is basically a power amplifier. However, regarding this thesis works concerns the proposed system will be rather termed as being a power generator or power converter. The reason for this distinction is that of the usual understanding a power amplifier often satisfies some expectations such as fidelity and linearity. Fidelity is about the amplifier being faithful to the signal it is being driven and linearity is the expectation from the amplifier that it should not change its respond properties, especially the gain value with the changing frequency of the input signal.

However to excite a laser it is not necessary to have the output signal to be an exact replica of the input feed or most of the circumstances the amplifier will or should stick to a single convenient frequency. Even more the harmonic content, distortion, phase or modulation noise of the output is not the criteria of the great importance for the desired system.

The power amplifier for a CO_2 laser application or similar applications such as RF heating, RF spark, arc or plasma generation and communications jamming should better be efficient, cost effective since usually extremely high powers are necessary.

3.2.1 Power Amplifiers: Classes of Operation

Although they all serve to supply gain to a proper input signal to generate a larger output signal, power amplifiers differ on their operation principles and are classified according to these principles. More specifically, the classification is based on the amount of time the output devices are conducting during one cycle of a periodic signal. There exist amplifiers in classes A, B, C, D, E, F, H, G, S, T and their combinations such as A/B and E/F. Besides there are some subcategories of operation modes such as, F_1 or F^{-1}.

Amplifiers of classes H, G, S, T and their mixtures will be omitted initially since they usually are not convenient for RF applications. These are advanced types of amplifiers, most of the times suitable for audio applications on fully digital systems. They also exploited for modulation and power or frequency conversion purposes. Class-H and class-G amplifiers have complicated structures with a series of power supplies attached. Class-S and Class-T amplifiers are the variants of class-D topology.

The rest can be divided into two basic categories. “The current source amplifiers” about classes A, B, C and A/B where the active device or devices serve as a current source control operated bellow the saturation level of the active device with the exception of saturated class-C operation. These amplifiers are typically described as "linear amplifiers" since their output voltage is proportional to the input signal. “The switch mode amplifiers” on which the active device or devices serve as an electric switch, being either one of the fully saturated on or off states.

An active device for an amplifier can be chosen out of many according to their properties, as it will be discussed among following sections. However an attention will be paid on MOSFET s for being the most cost effective alternative with

the highest power ratings for the frequency range of the applications interest. The proposed device for this thesis work will exploit MOSFET active device on a class-E configuration with in a combination of a matching network. In order to make the reasoning clearer other amplifiers of the different classes of operations will be discussed in brief.

3.2.1.1 Operation of Class-A

An amplifier operating in Class-A mode is biased such that the quiescent current is large enough that the transistor remains at all times in the active region and acts as a current source, controlled by the drive signal. In other words the active device is conducting all the times. The drain voltage and current waveforms are both sinusoidal on ideal conditions. The power output of an ideal class-A amplifier is,

$$P = V_{out} / 2R \tag{3.1}$$

where V_{out} the output voltage and R is the load impedance. The V_{out} can never exceeds Vdd the supply voltage. Power is dissipated even in the absence of an input signal. The DC-power input is constant and when there is no input signal, half of the maximum amount of drain current is dissipated by the output transistors.

It is only when there is some sort of input signal that some of the power is dissipated in the load rather than in the amplifier itself. Consequently, the instantaneous efficiency is proportional to the power output and the average efficiency is inversely proportional to the peak-to-average ratio.

The amplification process in class-A is inherently linear, hence increasing the quiescent current or decreasing the signal level monotonically decreases distortion and harmonic levels. Since both positive and negative excursions of the drive affect the drain current, it has the highest gain and fidelity of any amplifier.

The absence of harmonics in the amplification process allows class-A to be used at frequencies close to the maximum capability of the transistor. The on-state resistance or saturation voltage of the transistor degrades the efficiency of real class-A systems. It is also degraded by the presence of load reactance, which in essence

requires the amplifier to generate more output voltage or current to deliver the same power to the load.

However, the efficiency is low. Class-A amplifiers are therefore typically used in applications requiring low power, high linearity, high gain, broadband operation, or high-frequency operation.

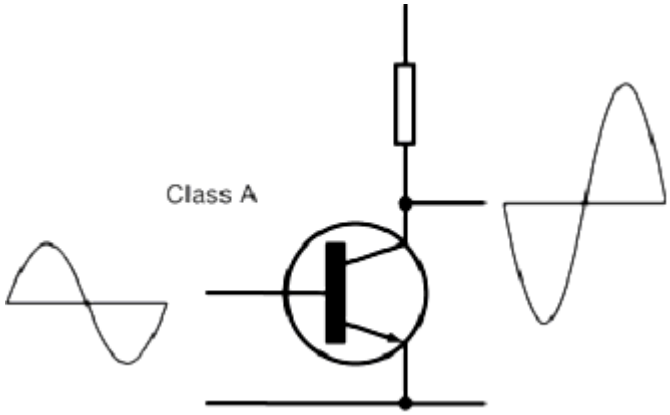

Fig 19. Class-A Amplifier

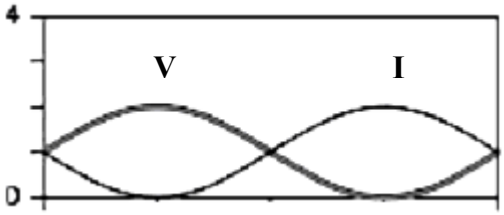

Fig 20. Ideal Waveforms of Class-A

3.2.1.2 Operation of Class-B

Class-B amplifiers are biased right at the threshold of conduction so that current flows in the output stage only when the input signal is greater than the turn-on voltage of the output transistors. As a result, the transistor is active half of the time and the drain current is a half sinusoid. Class-B provides linear amplification

and about 25% of improved efficiency, but suffer from higher levels of distortion, especially around the turn on point of the output transistors so called crossover distortion.

The drive level controls the power output of a class-B amplifier. The DC input current is, however, proportional to the drain current, which is in turn proportional to the RF-output current. Consequently class-B amplifiers are poor in fidelity.

The instantaneous efficiency of a class-B amplifier varies with the output voltage and for an ideal power amplifier reaches 78.5%. For low-level signals, class-B is significantly more efficient than class-A, and its average efficiency can be several times that of class-A at high peak-to-average ratios.

Class-B is generally used in a push-pull configuration so that the two drain-currents add together to produce a sine-wave output. It uses a complimentary pair of output devices and biases them such that they are never both on at the same time.

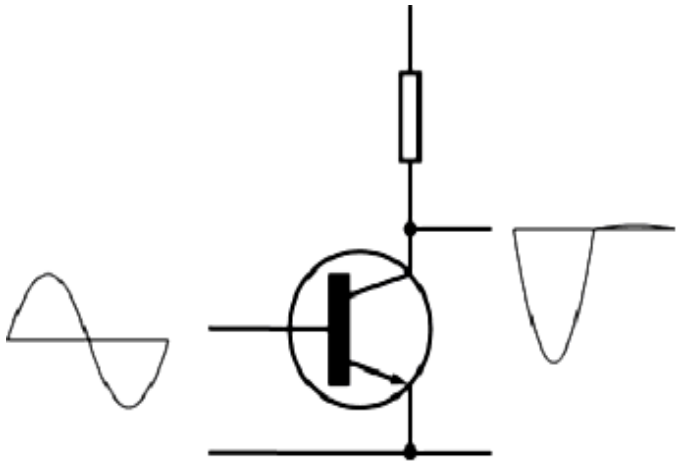

Fig 21. Class-B Amplifier

To produce a solution to crossover distortion is to bias the devices just on, rather than off altogether when they are not in use. This is called the class-A/B operation. Each device is operated in a non-linear region, which is only linear over half the waveform, but still conducts a small amount on the other half. The result is

that when the two halves are combined, the crossover is greatly minimized or eliminated altogether.

Class-A/B amplifiers would have some current flow with no input signal present since they are biased above the threshold voltage of the output stage. Class-AB amplifiers are better with linearity and fidelity but they have poorer efficiency.

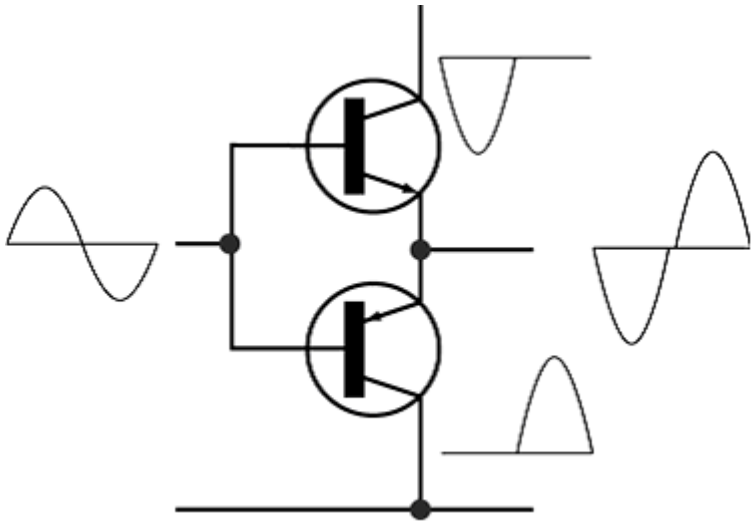

Fig 22. Class-B Push-Pull Amplifier

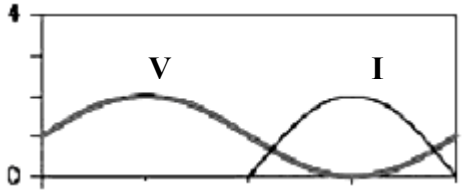

Fig 23. Ideal Waveforms of Class-B

3.2.1.3 Operation of Class-C

Class-C amplifiers are biased at zero volts, which is below the turn-on voltage of the output transistors. The input voltage must exceed the turn-on threshold of the output transistors before any current flows in the output stage. The active device is conducting for less than half of the RF cycle. The result is an amplifier with very high efficiency and very high distortion and loss of linearity. The output signal does not begin to rise until the input signal has exceeded the turn-on threshold.

A typical compromise is a conduction angle of 150° and an ideal efficiency of 85 percent. The output filter of a true class-C bypasses the harmonic components of the drain current to ground without generating harmonic voltages. When driven into saturation, efficiency is stabilized and the output voltage locked to supply voltage, allowing linear high-level amplitude modulation.

Classical class-C is widely used in high-power vacuum-tube transmitters. It is, however, little used in solid-state power amplifiers because it requires. low drain resistances, making implementation of parallel-tuned output filters difficult. With bipolar junction transistors, it is also difficult to set up bias and drive to produce a true class-C collector-current waveform.

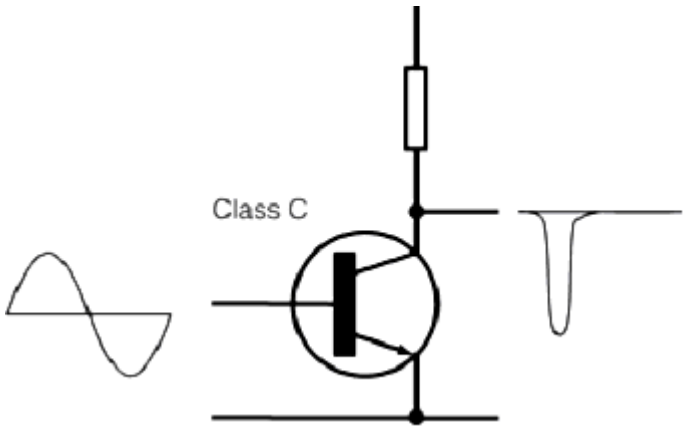

Fig 24. Class-C amplifier

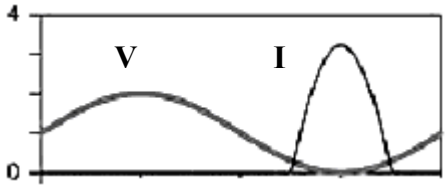

Fig 25. Ideal Waveforms of *Class-C*

The use of a series tuned output filter, results in a mixed-mode class-C operation that is more like mistuned class-E than true.
Class-C lacks of linearity and fidelity, but very successful to operate over a narrow band of frequencies.

3.2.1.4 Operation of Class-D

Class-D and beyond amplifiers are described as operating in "switch" mode. By operating the active device as a switch rather than a controlled current source, the voltage and current waveforms can, in principle, be made to have no overlap, reducing the theoretically achievable device dissipation to zero. At the same time, unlike class-C operation, the output power of switching modes can be comparable to or greater than that of class-A or class-B for the same device peak voltage and current.

The input signal is simply used to turn on the output stage transistor to its full output power. Once the input signal falls below the turn-off threshold, the amplifier output immediately falls to zero. The result is that the output waveform is typically a square-wave with an amplitude equal to the voltage placed across the output stage.

Class-D amplifiers use two or more transistors as switches to generate a square drain-voltage waveform. A series-tuned output filter passes only the fundamental-frequency component to the load. Current is drawn only through the transistor that is on, resulting in 100% efficiency for an ideal power amplifier.

A unique aspect of class-D is that efficiency is not degraded by the presence of reactance in the load. Practical class-D amplifiers suffer from losses due to saturation, switching speed, and drain capacitance. Drain capacitance must be charged and discharged once per RF cycle and finite switching speed causes the transistors to be in their active regions while conducting current often referred as cross conductance.

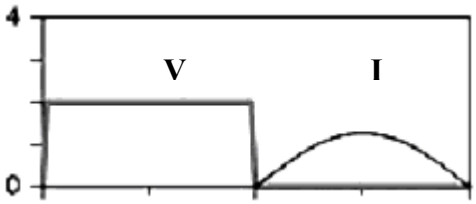

Fig 26. Ideal waveforms of Class-D

Such various problems cause inefficient operation trough high frequencies over 3Mhz. To overcome cross conductance, a portion of the duty cycle is sacrifice to introduce dead times trough switching.

The ideal outputs of class-D amplifiers are being the square waves may be noted as a draw back of this topology.

3.2.1.5 Operation of Class-E

In Class-E amplifiers, the output stage is designed into a special filter circuit that converts the square-wave into a sine wave with a great deal of efficiency. . The drain voltage waveform is the result of the sum of the DC and RF currents charging the drain-shunt capacitance. A perfectly designed Class-E amplifier will have no voltage across the output stage transistors while current is flowing in that transistor. The drain voltage will fall to zero and has zero slope just as the transistor turns on. Since there is no voltage drop, no power is dissipated in the output stage. Class-E amplifier can practically operate at efficiencies approaching 100%.

Class-E employs a single transistor operated as a switch. Class-E topology eliminates the losses associated with charging the drain capacitance in class-D, reduction of switching losses, and good tolerance of component variation. Variations in load impedance and shunt susceptance cause the power amplifier to deviate from optimum operation, but the degradations in performance are generally no worse than those for class A and B.

As mentioned above, Class-E amplifiers have very high efficiency and are capable of producing sine-wave output signals. Additionally, since no power is dissipated in the output stage during switching, the output stage requires minimal heat sinking. This is a distinct advantage since most linear amplifier requires very large heat sinks.

A disadvantage of Class-E amplifiers is that the output signal amplitude is independent of the input signal amplitude, but followed with the advantage that amplitude of the input signal does not have to be carefully controlled, so simple digital signals can be used. The output power can be simply controlled by controlling the voltage across the output stage of the amplifier. Another disadvantage of Class-E amplifiers is that, because of the tuned filter in the output stage, the amplifiers have a much narrower bandwidth than linear amplifiers. The Q of the tuned filter limits the bandwidth of a Class-E amplifier. The use of multiple filter circuits that are switched in and out of the circuit can increase the bandwidth of the amplifier, but at the expense of size.

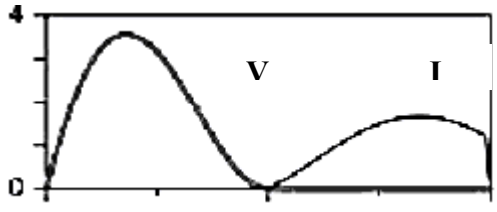

Fig 27. Ideal waveforms of Class-E

3.2.1.6 Operation of Class-F

The Class-F operation has been developed primarily as a means of increasing saturated performance of class-AB and class-B designs. As a result, the attainable operating frequencies are higher than those for class-E circuits, but the performance limitations due to the tuning requirements and the lack of a simple circuit implementation, suitable for nearly ideal switching, make class-F a poor alternative at frequencies where a lumped-element class-E can be implemented.

They increase both efficiency and output by using harmonic resonators in the output network to shape the drain waveforms. The voltage waveform includes one or more odd harmonics and approximates a square wave, while the current includes even harmonics and approximates a half sine wave. Alternately "inverse class-F", the voltage can approximate a half sine wave and the current a square wave. As the number of harmonics increases, the efficiency of an ideal power amplifier increases from the 50 percent that of a class-A toward unity.

The required harmonics can in principle be produced by current source operation of the transistor. However, in practice the transistor is driven into saturation during part of the RF cycle and the harmonics are produced by a self-regulating mechanism similar to that of saturating class-C. Use of a harmonic voltage requires creating high impedance at the drain, while use of a harmonic current requires low impedance.

While class-F requires a more complex output filter than other power amplifiers, the impedance must be correct at only a few specific frequencies. A variety of modes of operation in-between class-C, E, and F are possible.

Apart from the widely used class-C, class-E and class-F amplifiers seems to be better candidates in order to be used with CO_2 lasers. Comparing class-E to the two class-F tunings, several advantages of the former are apparent.

Class-E has the advantage of being capable of strong switching operation even with a very simple circuit, whereas class-F allows this only as a limiting case using a circuit with great complexity. Class-E amplifier is limited only by the intrinsic switching speed of the active device, whereas class-F amplifier tunings may

find their switching speed dominated by the limited number of harmonics, which have been utilized in the waveforms. Additionally, class-E has the advantage of incorporating the output capacitance of the transistor into the circuit topology.

The class-E tuning not only absorbs the capacitance into the basic network, but also allows zero voltage switching "ZVS" operation, eliminating discharge losses from this capacitor. The tuning of class-E circuits is also very simple, requiring only one parameter to be adjusted to achieve high-efficiency ZVS operation.

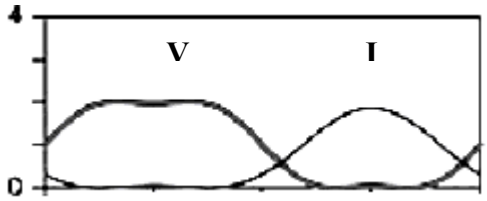

Fig 28. Ideal waveforms of Class-F

3.2.2 Detailed Discussion of Class-E Operation

Although Class-E amplifier design is first explored by Gerard Ewing in 1964, Sokal A. D. and Sokal N. O. first presented it in 1975 [35] and patented. As stated earlier, a class-E is nonlinear amplifier, in the sense that variations in input signal amplitude will not reproduced at the output in any acceptable form. Moreover, class-E configurations prove to have higher efficiency with simpler circuits than conventional reduced conduction angle classes.

Following the original notation, a basic class-E amplifier is composed of an active device switch Q_1, a choke inductor L_1, a shunt capacitor parallel to the switch C_1, a resonant circuit inductor L_2, a DC blocking capacitor C_2 and the load R. The transistor switch Q is ON in half of the period, and OFF in the other half.

In most RF and microwave power amplifiers, the largest power dissipation is in the power transistor. The product of simultaneous voltage and current integrated and averaged over the RF period gives out the power dissipated on the active device.

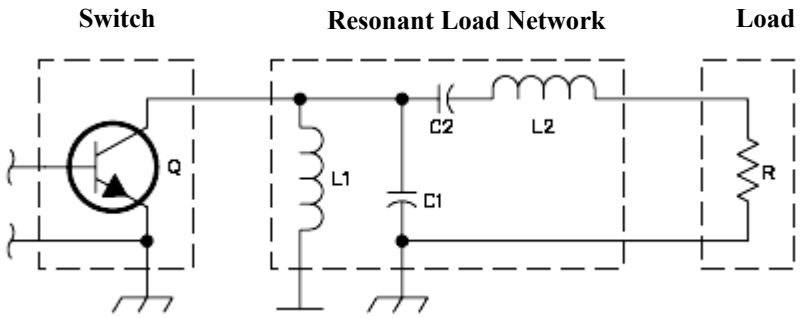

Fig 29.Low Order Class-E Amplifier [35]

The active device must sustain high voltage during part of the RF period and conduct high current during part of the RF period, however the circuit can be arranged so that high voltage and high current do not exist on the active device simultaneously. Then the product of active device voltage and current will be low at all times during each RF cycle.

In the ideal situation, the efficiency of a class-E amplifier is 100%. However, in practice, the switch has a finite on-resistance, and the transition times from the off-state to the on-state and vice- versa are not negligible. Both of these factors result in power dissipation in the switch and reduce the efficiency. To achieve the most efficient operation following conditions are necessary to be fulfilled by the circuit trough each RF cycle. These conditions stated by Sokal N. O. [28][35];

1. When the active device is ON, the voltage is nearly zero and high current is flowing.

2. When the device is OFF, the current is zero and there is high voltage. The transistor acts as an open switch.

3. The rise of transistor voltage is delayed until after the current has reduced to zero.

4. The transistor voltage returns to zero before the current begins to rise.

5. The transistor voltage at turn-on time is nominally zero.

6. The slope of the transistor voltage waveform is nominally zero at turn-on time.

These conditions are stated in order to avoid;

1. The simultaneous existence of current and voltage on the active device
2. Losses due to active device switching times, which will, unavoidably, be appreciable fractions of the RF period.
3. Dissipating the stored energy on capacitor C_1.
4. Uncontrolled sharp rise of the current injected to turn-on active device by the load network while the active device conductance is building-up from zero during the turn-on transition.

Followed by the satisfaction of these conditions, the voltage and current switching transitions are time-displaced from each other in order to accommodate transistor switching transition times that can be substantial fractions of the RF period. Turn-on transitions may be up to about 30% of the period and turn-off transitions up to about 20% of the period [28].

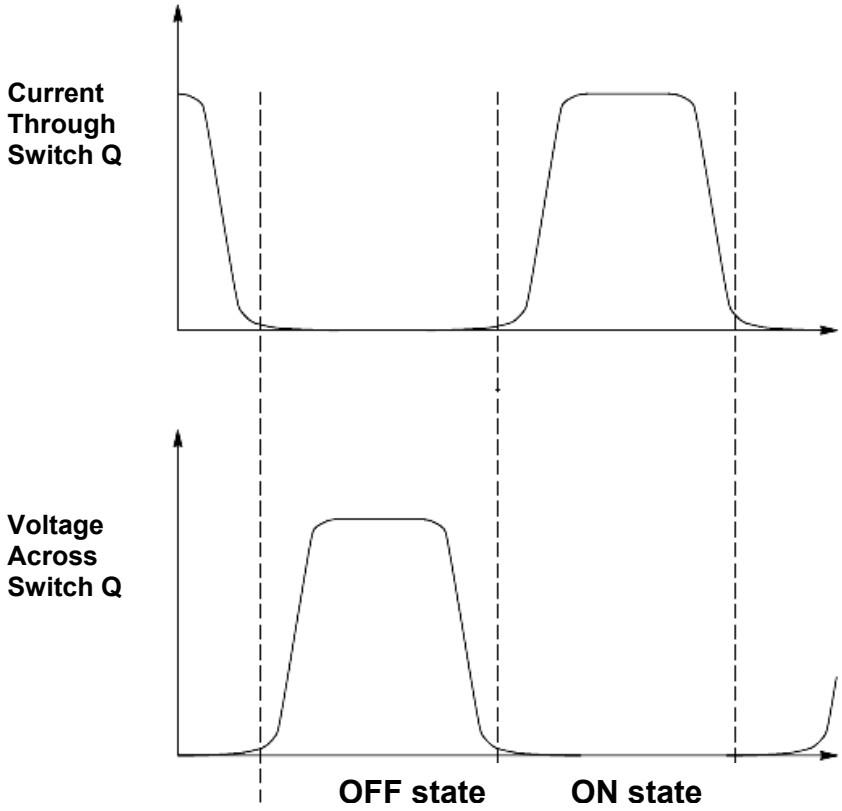

Fig 30. Conceptual "target" waveforms of transistor voltage and current [35].

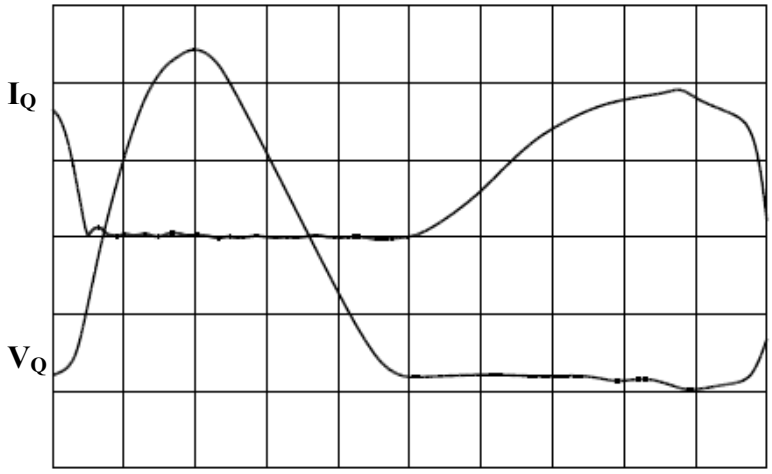

Fig 31. Actual transistor voltage and current waveforms in a low-order Class-E amplifier [28].

3.2.3 Numerical Implementation of Class-E Operation

The analysis of the class- E amplifiers has been reported in several papers, especially on mostly cited papers by Sokal 1975 [35], F. Raab 1978 [34] and Kazimierczuk 1983 [32].

3.2.3.1 The Load Network Quality Factor

Analytical derivations of design equations for the low order class-E operation can be made only by assuming the current in *L2* and *C2* is sinusoidal. That assumption is strictly true only if the load network has infinite loaded quality factor "Q_L",

$$Q_L = \frac{\omega L_2}{R} \tag{3.2}$$

Q_L values progressively lower than infinity yields progressively less-accurate results. Q_L is a free-choice design variable, subject to the condition,

$$Q_L \geq 1.7879 \tag{3.3}$$

obtained from exact numerical analysis. The maximum possible value should be less than the network's unloaded Q_L. This value determines the lowest value to obtain the nominal switch-voltage waveform, for the usual choice of the switch ON duty ratio"D"; $D = 50\%$.

The amplifier's output power "P" can also be derived from exact numerical analysis and depends primarily on the collector/drain DC-supply voltage V_{dd} here after, and the load resistance R, but secondarily on the value chosen for QL. This last statement is not derivable from exact numerical analysis.

Similar restrictions apply to the analytical derivations of design equations for C_1, C_2 and R. However, the needed component values can be found by numerical methods. Sokal [28] explained normalized exact numerical solutions for output power and the needed value of R, $C1$ and $C2$, for eight values of QL over the entire possible range from 1.7879 to infinity, for the usual choice of D = 50%.
Kazimierczuk and Puczko [32] published a similar tabulation to, but they did not include continuous-function design equations based on their tabular data. Precise design values cannot be read from the graphs. To make accurate circuit designs and advance design evaluations at any arbitrary value of Q_L, one needs design equations comprising continuous mathematical functions rather than a set of tabulated values.

The choice of Q_L involves a trade-off among operating bandwidth, harmonic content of the output power and power loss in the parasitic resistances of the load network inductor L_2 and capacitor C_2. A lower value for Q_L leads a wider bandwidth and decreased power loss due to the parasitic resistances of the network components, whereas a higher value for Q_L leads lower harmonic content delivered to the load.

Reference [35] pointed similar aspects of the choice of Q_L value, that it will determine the degree of damping trough the network. Too low Q_L value, consequently too much damping will disable the voltage across C_1 returning to zero and therefore the uncharged power will be dissipated on active device. With too high Q_L, consequently too little damping, the voltage across the active device will swing below zero resulting an inverted mode. It is useful to note here that, MOSFETs contain a commutation diode between the drain and the source, preventing the device from damaging on inverted operation.

Q_L	$\frac{PR}{(V_{CC}-V_o)^2}$	$C1 \bullet 2\pi fR$	$C2 \bullet 2\pi fR$
infinite	0.576801	0.18360	0
20	0.56402	0.19111	0.05313
10	0.54974	0.19790	0.11375
5	0.51659	0.20907	0.26924
3	0.46453	0.21834	0.63467
2.5	0.43550	0.22036	1.01219
2	0.38888	0.21994	3.05212
1.7879	0.35969	0.21770	infinite

Table 2. Dependence of P, C1, and C2 on loaded Q_L [28]

3.2.3.2 The Supply Voltage

Due to the nature of the load network, a potential of peak to peak maximum of 3.56 times the applied voltage can be generated across the active device. Obviously this potential should be limited within the absolute maximum ratings of the active device to be used. In case of MOSFETs this rating is given with the notation V_{dss} on manufacturers datasheets. An explicit formula for the voltage to be applied can be expressed as follows,

$$V_{dd} = \left(\frac{V_{dss}}{3.56} \right) SF \tag{3.4}$$

Here *SF* represents the safety factor, a choice of design should be lower than unity. SF is necessary to allow for higher peak voltage resulting from off-nominal load impedance. Due to the nature of the plasma applications this value should be determined carefully. Although the impedance matching circuitry would try to adjust itself to the load mismatch conditions, especially followed by ignition, system possibly would not react fast enough.

3.2.3.3 Power, Load and Efficiency Considerations

The relationship among P, R, Q_L, and V_{DD} is calculated from exact numerical analysis. Originally such equations should contain a value for the active device saturation offset voltage V_0, however the discussions on this thesis work is limited with MOSFETs and for the MOSFETs case V_0 value is negligible. Following equations are found to fit the tabulation given on table 2 [28], over the entire range of Q_L from 1.7879 to infinity, within a deviation of ±0.15%, by a second-order polynomial function of Q_L. Likewise a third order evaluation will yield a deviation of –0.0089% to +0.0072% and so on, all of which are well below the available passive component tolerances.

The second order function of Q_L is expressed as,

$$f(Q_L) = 1.001245 - \frac{0.451759}{Q_L} - \frac{0.402444}{Q_L^2} \tag{3.5}$$

and the third order function of Q_L is,

$$f(Q_L) = 1.0000086 - \frac{0.414395}{Q_L} - \frac{0.577501}{Q_L^2} + \frac{0.205967}{Q_L^3} \tag{3.6}$$

also a useful simplification on the exact numerical analysis should be to noted;

$$\frac{2}{\frac{\pi^2}{4}+1} = 0.576801 \tag{3.7}$$

Finally the relations on R and P expressed as follows,

$$P = 0.576801\frac{V_{dd}^2}{R} f(Q_L) \tag{3.8}$$

Equation (3.8) informs us about the power and load relation on ideal conditions. Nevertheless a real amplifier will be composed of non-ideal components and decrease the efficiency from 100%. The effects of non-ideal components may be absorbed in to the R-value of the load,

$$R_{load} = R - ESR_{L2} - ESR_{C2} - 1.365R_{on} - 0.2116ESR_{C1} \tag{3.9}$$

where *R*on is the "on" resistance of the transistor. "*Ron"* is a generic term that represents "$R_{DS(on)}$" of a MOSFET given in manufacturers datasheets. "*ESR"* is the effective series resistance of a reactive component.

While considering the efficiency due to non-ideal components it is also necessary to define a constant for switching transition duration, which will unavoidably occupy a fraction of a RF cycle. Such a constant is given on reference [45],

$$A = t_f f\left(1+\frac{0.82}{Q_L}\right) \tag{3.10}$$

where t_f is the 100%-to-0% fall time of the assumed linear fall of the drain/collector current at transistor turn-off.

Another source of power loss factor is the DC and RF resistances of the DC-feed choke L_1, may be accounted to have an effect of 1% efficiency loss.

Together these effects of non-ideal components with the R-value obtained from equation (3.8) are exploited to give a definition for efficiency,

$$\eta = \frac{R_{load}}{R_{load}+ESR_{L2}+ESR_{C2}+1.365R_{on}+0.2116ESR_{C1}} - \frac{(2\pi A)^2}{12} - 0.01 \tag{3.11}$$

VDS	Id	Po	Vdrain	Efficiency	PS load line
V	A	W	Vp	%	Ω
89.7	1.40	100	231	79.6	64.1
128.4	1.86	200	334	83.7	69.0
157.5	2.23	300	411	85.4	70.6
181.7	2.56	400	476	86.0	71.0
203.4	2.86	500	534	85.9	71.1
222.9	3.13	600	588	86.0	71.2
241.1	3.39	700	636	85.6	71.1
257.9	3.63	800	683	85.5	71.0
273.8	3.85	900	723	85.4	71.1
289.1	4.07	1000	763	85.0	71.0

Table 3. Consequences of the supply voltage variation on operation parameters [44]

3.2.3.4 Determination of Passive Component Values

A discussion on component values should start with L_1 the DC feed choke. Since none of them will operate ideally, it will present a portion of susceptance and will have minor effects on other system parameters. Reference [35], where the class-E operation is first presented, the L_1 is described to be a high reactance DC feed choke, sufficiently large enough to act as a source of substantially constant current. The practical implementation would allow any one of the commercially available components, capable of operating at desired frequencies.

Determination of L_2 is straightforward and in fact was mentioned on the definition of Q_L. Hence a new equation for L_2 can be expressed as,

$$L_2 = \frac{Q_L R}{\omega} \tag{3.12}$$

Necessary data to calculate values for $C_1$and C_2 was given on table 2. Choosing the desired Q_L value out of several alternatives, values for C_1 and C_2 can be found. Yet more precise values can be obtained via equations from the exact numerical analysis, including the effects of L_1,

$$C_1 = \frac{1}{\omega R\left(\frac{\pi^2}{4}+1\right)\frac{\pi}{2}}\left(0.99866+\frac{0.91424}{Q_L}-\frac{1.03175}{Q_L^2}\right)+\frac{0.6}{\omega^2 L_1} \text{ [28]} \tag{3.13}$$

$$C_2 = \frac{1}{\omega R}\left(\frac{1}{Q_L-0.104823}\right)\left(1.00121+\frac{1.01468}{Q_L-1.7879}\right)-\frac{0.2}{\omega^2 L_1} \text{ [28]} \tag{3.14}$$

Since the component values of the class-e operation are all depended on each other due to the Q_L parameter, there are many ways to generate formulas for the calculation of the component values. A good example is, on their work authors of [32] also accounted for the Q_L parameter to be,

$$Q_L = \frac{1}{\omega RC} \tag{3.15}$$

based on the value of the tank capacitance.

It is also possible to deviate more plain formulas for the network components considering the frequency range that it will be utilized. For instance working beyond UHF ranges and through microwaves makes it essential to account for the parasitic effects and non-linear behavior of the components. A similarly lower frequency of the kHz range increases the usable margins.

Most of the resources about the calculation of class-E component values are related to the efforts at lower microwave levels on digital communication purposes due to the industries great interests. Yet others spend much of their efforts for component values allowing much more broad bandwidth still avoiding further harmonics.

Followed by the determination of the V_{dd} and power and Q_L parameters, it should rather be a wiser choice to stick on some proper capacitance values of the industry standard and leave others to be calculated based on this certain values.

It is also necessary to note that all the previously given formulation are valid under the assumption that the designer will make the proper choice of the duty factor of 50%. Exact numerical analysis with varied duty cycle ratios are presented by the authors of [32]. However besides the technical problems introduced with varying duty ratios, a 50% ratio is stated to be the most optimal one.

3.2.3.5 Tuning Procedure

None of the previous discussions mentioned about the load possessing reactive components. This was explained on reference [35]. Firstly the impedance values about the operational frequency should be taken into the account. Influences of the harmonics are stated to be negligible. Than the designer will make the assumption that, any series inductive reactance adds to that of L_2 and any series capacitive reactance adds to that of C_2. Then the circuit would operate with an off-nominal voltage waveform and possibly an off-nominal value of output power, because the effective values of *L2* and *C2* differ from the design values. The reactances of *L2* and *C2* should be reduced by the amounts of the residual reactance

at the matching network input in order provide nominal operation. The designer has the information of how to align back to nominal operation values exploiting the formula presented previously. However most of the times, especially while dealing with the plasma as a load, proper values to be subtracted from nominal design parameters are unknown.

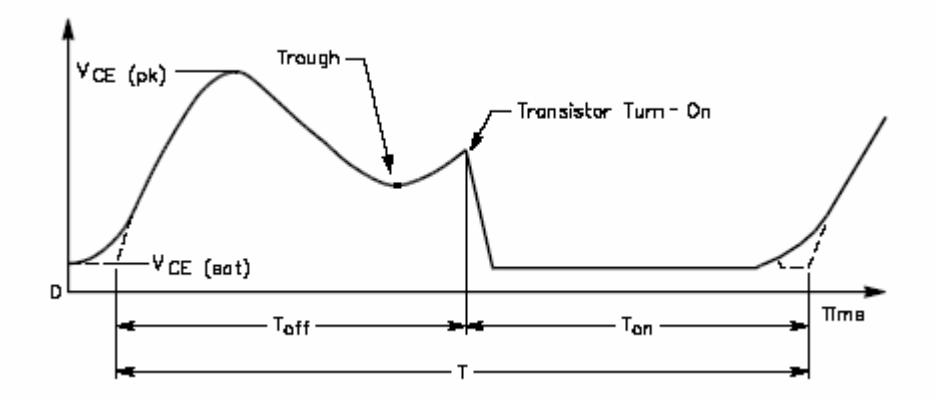

Fig 32. Typical waveform showing the active device turn-on, turn-off and waveform trough due to mistuning [28].

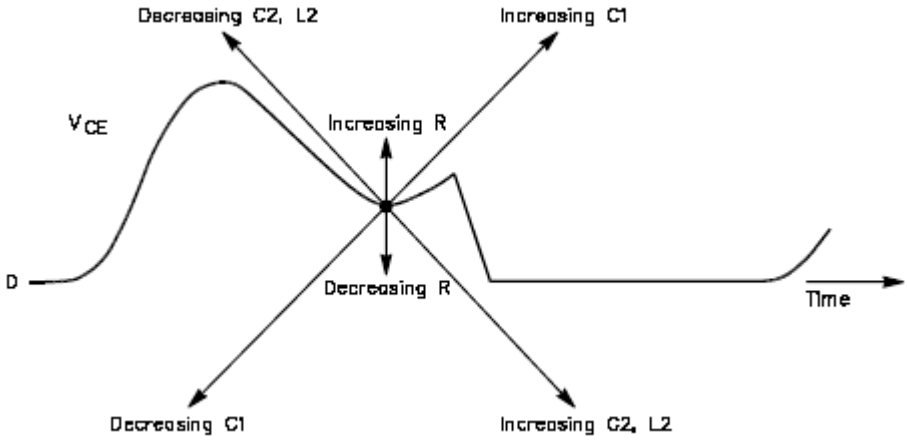

Fig 33. Effects of load network components alignments [28].

The tuning procedure should not depend on input and output power considerations [36]. Alternatively a tuning procedure can be followed observing the

waveform across the active device. The nominal waveform was presented on figure 31. Adjustments can be performed aiming to reach the nominal waveform using the knowledge gathered. Increasing *C1* moves the trough of the waveform upwards and to the right while increasing *C2* moves the trough of the waveform downwards and to the right. Increasing *L2* moves the trough of the waveform downwards and to the right. It will also be noted that increasing L2 will result a decrease on power output. Increasing *R* moves the trough of the waveform upwards.

3.2.3.6 Effects of Load Variations

Uncontrolled load variation is possibly the most apparent problem to be handled in order to utilize the class-E operation coupled to a plasma application with or with out an impedance matching assistance. The load and the variation due to the load is not necessarily an ohmic resistance. For any given plasma application reactive components are also involved.

Resistive component of the load when varied affects the power, efficiency and the voltage across the active device as well. Derived from the exact numerical analysis, efficiency varies gradually, remaining at 95% or more for variations in the load resistance of +55% to –37%. Variation of both input and output power is also gradual. For load resistances smaller than the ideal value, the voltage across the active devices swings both to a more negative and to more positive value.

As stated earlier, reactive components of the load are accounted to be absorbed in to the load network elements. Deviations on the reactance of the load, consequently mistuning of the series tuned load network causes a change in the load angle φ. Again implementation of the exact numerical analysis show that the nominal operation parameters are reached within a range of 49˚ to 65˚ of the load angle. They are also found to be still tolerant to variations in between 40˚ to 70˚ [31].

Table 3 lists the results of an experiment conducted at 13.56 MHz with a class-E amplifier of 1kW demonstrating effects of severe load variations on various parameters of the operation. Resistance of the load is varied by a factor of ±10. It is interesting to note that variations of the increased resistance types are introducing

more worrying consequences. Whereas a severe fall of the load resistance forces the limits of the active device about the voltage levels it can withstand.

Reference [33] suggests prevention against load variations. To keep the class-E circuitry operation at maximum efficiency a series of load networks are proposed. These networks can be switched by means of high frequency relays again under automatic control to adopt load variations. An optimal value for the frequency of the operation is calculated for each network option. Thus the frequency will also be switched simultaneous again under automatic control.

R_{LOAD}	Vds pk	Ids pk	Pout	Pin	Ploss	Eff %	REMARKS
1.25Ω	923V	18.7A	187W	333W	146W	56%	Low
12.5Ω	808V	16.4A	1003W	1134W	131W	88.4%	Normal
125Ω	636V	32A	359W	1116W	757W	32%	High

Table 4. Consequences of the load variation on operation parameters

3.2.3.7 Harmonic Content

The harmonic content of the power produced by a class-E amplifier is obviously dependent of the Q_L value of the load network. However as stated previously chosen the higher value of Q_L will sacrifice the output power capabilities of the given arrangement.

Raab and Sokal explained the harmonic content of the power produced by a class-E amplifier on their manuscript [36]. The ratio of I_n the current due to the n^{th} harmonic to I_1 the current at the fundamental frequency is tabulated as a function of Q_L. Q_L values of a class-E operation bellow 1.7879 are banned.

However the for Q_L value of 2, the current ratio of the second is tabulated to be 0.602, which apparently is not negligible. Although the design criteria seems to

be in favor of selection of lower Q_L values, effects of harmonic content should be regarded.

3.2.3.8 Exact Numerical Analysis

Detailed exact numerical analysis of class-E operation is given by Raab [34], Kazimierczuk and Puczko [32]. Some different other analysis techniques are also possible. Raab conducted his analysis from the characteristics of the steady-state operation. He assumed that the Q_L value is high enough that the signal is essentially a sinusoid. He also assumed an ideal switch and ideal passive components.

Ideally sinusoidal output voltage and current can be expressed as,

$$V_0(\theta) = c\sin(\omega t + \varphi) = c\sin(\theta + \varphi) \tag{3.16}$$

$$I_0(\theta) = \frac{c}{R}\sin(\theta + \varphi) \tag{3.17}$$

Since the DC feed choke forces a DC current and the series network forces a sinusoidal, their difference flows in to the switch and shunt capacitor combination. When the switch is on the current difference flows through the switch and when of into the shunt capacitance. Thus, if the voltage across the shunt capacitor is not zero at the moment switch returns to ON value then, it will discharge through the switch dissipating capacitor energy. Similarly by the time the switch is OFF, a voltage is produced across the switch with the discharging capacitor, that is,

$$V(\theta) = \frac{1}{C\omega}\int_{\theta_0}^{\theta} I_c(u)du \;\; Q_2 = \frac{\omega_{02}L}{R} = \omega_{02}R\frac{C_2C_1}{C_2 + C_1} \tag{3.18}$$

At the fundamental frequency the load network should have zero voltage drop across it, thus (3.18) should be equal to the hypothetical voltage of the circuit. The hypothetical voltage will differ from the output voltage given (3.16) for their phase difference due to the reactance possessed,

$$V(\theta) = V_0(\theta) + V_x(\theta) \tag{3.19}$$

$$= c\sin(\theta + \varphi) + X\frac{c}{R}\cos(\theta + \varphi) \tag{3.20}$$

$$= c_1\sin(\theta + \varphi_1) \tag{3.21}$$

where,

$$c_1 = c\sqrt{1+\frac{X^2}{R^2}} \tag{3.22}$$

and,

$$\varphi_1 = \varphi + \psi = \varphi + \tan\left(\frac{X}{R}\right) \tag{3.23}$$

These relations are further computed exploiting Fourier analysis to supply the basis for the discussions of the previous sections.

It should be noted that exact numerical analysis by Raab did not involved the effects of variable Q_L and switch duty cycle D. An analysis including these variables introduced by Kazimierczuk and Puczko [32]. They only made assumptions for the ideal components.

Kazimierczuk and Puczko noted that in fact there exists two different resonant frequencies and two different Q values for this resonant conditions according to the condition of the switch, whether it is ON or OFF. Thus when the switch is ON,

$$\omega_{01} = \frac{1}{LC_2} \tag{3.24}$$

$$Q_1 = \frac{\omega_{01}L}{R} = \frac{1}{\omega_{01}RC} \tag{3.25}$$

and when the switch is OFF,

$$\omega_{02} = \frac{1}{\sqrt{\frac{LC_2C_1}{C_1+C_2}}} \tag{3.26}$$

$$Q_2 = \frac{\omega_{02}L}{R} = \omega_{02}R\frac{C_2C_1}{C_2+C_1} \tag{3.27}$$

also through interpretation of the steady-state wave forms two distinct cases, underdamped and overdamped conditions are regarded. Solving the waveforms due to these criteria, they have produced tabulations of amplifier parameters and component values for different Q_L values ranging from 0 to 100 and different duty cycles of 0.25 0.50 and 0.75.

Further analyses by various authors are also available mainly in order to make clearer the effects of non-ideal components.

3.3 Impedance Matching

Both numerically and empirically it is proven that in or to deliver maximum power achievable to the load, source and load impedance's should be matched. In other words their real internal resistances should be seen equal by each other and reactance's should be cancelled. Consequently, while reaching to the load, voltage and current components will be of the same phase dissipating all the power on the load.

The impedance of the plasma is changing continuously because the dielectric aspects of the plasma are being altered by changes in the temperature, pressure, and dielectric constant of the plasma. Therefore, the changing RF load impedance must be continuously matched to the RF source.

3.3.1 Standing Wave Ratio

A standing wave on a transmission line can be thought of as being composed of two traveling waves, one moving toward the load, the forward wave and one moving in the opposite direction, the reflected wave. These waves, moving through the transmission path, interfere with one another to produce the standing wave. Each of these waves have a voltage amplitude, the forward voltage V_f and the reflected voltage V_r. The standing wave ratio "SWR" and the "Γ " the complex reflection coefficient are defined to manage this concept.

$$SWR = \frac{1+|\Gamma|}{1-|\Gamma|} \tag{3.28}$$

$$|\Gamma| = \frac{SWR-1}{SWR+1} \tag{3.29}$$

In many situations, a good match is defined arbitrarily as having SWR<1.5. From the following table, one can see that the reflected power from the mismatch

becomes of the same order of magnitude as the incident power at SWR 1.5, although in many situations we require return loss greater than 30 dB, which corresponds to SWR=1.07.

SWR	$\lvert\Gamma\rvert$	Return loss dB	$1-\lvert\Gamma\rvert^2$	Transmitted loss dB
1	0.00		1.00	0.00
1.05	0.02	32.3	1.00	0.00
1.1	0.05	26.4	1.00	0.01
1.2	0.09	20.8	0.99	0.04
1.5	0.20	14.0	0.96	0.18
2	0.33	9.5	0.89	0.5
3	0.50	6.0	0.75	1.25

Table 5. SWR related parameters

Standing waves, in case they are not dissipated on the load are not necessarily dissipated back on the source. For the case of the open lossless line, there is no power lost in the load, line, or the generator, and so there is no real power lost anywhere, but there are forward and reflected power figures.

3.3.2 Matching Techniques

There are several practical techniques employed by engineers, such as quarter-wave transformers, stub tuners, double stub tuners, and lumped component networks. However with the characteristics of the impedance variation of the plasma-based system, lumped component networks are the only feasible solution. Lumped component networks can be made up of varying impedance components that give them the ability to match varying loads.

Other matching techniques work better with fixed load because their matching abilities are related to lengths and configurations, which are not easily varied. Another consideration is that it is better that lumped component networks be made of only reactive elements, since reactive elements do not waste as much energy

as resistors in the form of heat and noise. The other advantage of the matched load condition is that it uniquely removes the requirement for a specific reference plane.

Lumped component networks have various types and possible cascaded configurations. Cascaded configurations are rather useful when they are exploited as filters. However, to be used with a plasma application they should be as simple as possible, not loosely and easily adjustable. Of the common practice Π- L- and T-types are used on their low pass configurations.

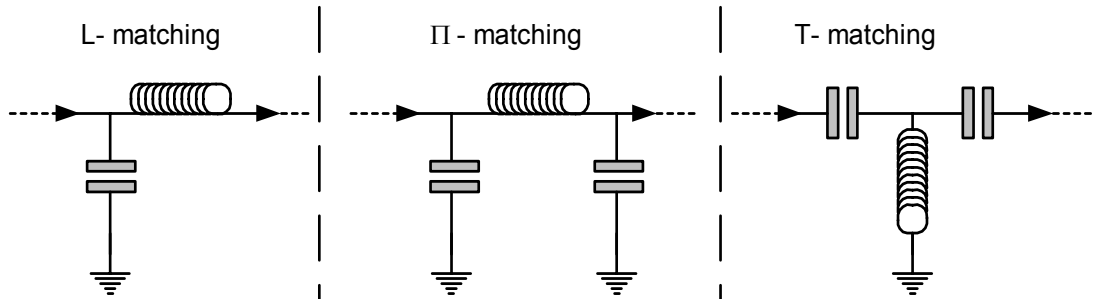

Fig 34. Feasible impedance matching networks

The goal of the matching network is to eliminate mismatch on the source side of the matching network, thus maximizing the power delivered to the load. However stability is another issue of which the impedance matching system is responsible. Stability is a factor of the reaction time of the impedance matching system to the altering plasma conditions. If this process were automated, the dependency on the operator of the system would be eliminated. Consequently more stable more repeatable operations will be obtained.

An automated system may measure one or more of the several parameters about the running operation and may exploit these data to recalculate or seek for better impedance matching conditions. The automated system can reconfigure the matching system by mechanical or electronic means or both. Such a system will be qualified according the time it has to spend on adapting to the altering plasma conditions.

An automated impedance matching system may use the amount of power dissipated, the phase difference between voltage and current components and the standing wave ratio as feedback data. Although there exists some other methods to supply information about the active medium impedance, those are relatively complicated to be employed with an automatic impedance matching system.

3.3.3 Determination of the Plasma Impedance

Whether with an automated or manual impedance matching, to determine the initial conditions before the ignition of the plasma or to take action against altering plasma conditions, plasma impedance or indirect consequences of plasma impedance should be known. There are several practically manageable methods to gather this knowledge depended on empirical. Whereas numerical calculations usually would not be satisfactorily accurate since the system is composed of non-ideal components and yet the nature is not fully understood.

One of these methods is making use of voltage and current probes; the voltage over and current through the reactor can be measured, along with their relative phase difference. With this voltage, current, and phase difference, the reactor impedance can be measured.

Another one is to exploit matching network settings for the situation in which the discharge impedance is matched to the RF power source; the discharge impedance can be calculated. For this calculation, all the components in the circuit, including the stray impedance's, have to be known. The key point of this method is that, if the network is matched, then the total impedance of the matchbox and the reactor is equal to the internal impedance of the power source.

A third method is not very different from the second one. First, the matching network is tuned correctly. After this, the discharge is extinguished, and the RF power source is replaced by impedance, which has the same value as the RF power source's internal impedance. Then a network analyzer is connected to the RF electrodes, and the impedance of the network is measured. When the losses in the matching network are negligible, this measured impedance is equal to the complex

conjugate of the discharge impedance. No knowledge of the component values in the matching network is needed for this technique to work.

The advantage of the first two methods is that the impedance can be measured when the discharge is on. Both first two methods are real-time and non-intrusive. For the usage of the third method, however, the discharge has to be extinguished before the impedance can be measured. A disadvantage of the first two methods is the fact that the stray impedances in the network have to be known. For the usage of the third method, these impedances need not be known.

Alternatively an exact knowledge of plasma is not acquired. In order to match a varying impedance load, the amount of forward and reflected power can be quantified. This can be done using a directional coupler. A directional coupler samples the RF waves traveling through the system and rectifies them by use of diodes and capacitors. The diodes are placed in the circuitry in two different polarities in order to detect both forward and reflected traveling waves. The total voltage on the line can be equated to the sum of the incident (forward) and reflected waves,

$$V(z) = V_0^+ e^{-j\beta z} + V_0^- e^{j\beta z} \tag{3.30}$$

thus the small voltage values that are attained from diode circuitry are proportional to the forward voltage and the reflected voltage value on the line. The rectified voltage values are directly proportional to the amount of forward and reflected power experienced in the system. These respective voltage values can be divided to produce the magnitude of the reflection coefficient.

$$\left|\Gamma\right| = \frac{V_0^-}{V_0^+} \tag{3.31}$$

3.3.4 Determination of Component Values

In determining the values of the reflection coefficient to be compared and tested against, the maximum VSWR allowed, 1.1 to 1 is used. This value relates to a reflection coefficient of 0.04762. To achieve this dumped network components

should be determined with in a tolerance and will be adjusted to their necessary values.

There are several ways to supply impedance matching with reactive networks. Manual computations are not easy to handle. Computations are tedious due to the length of the equations and the complex nature of the numbers is required to be manipulated. The designer may benefit computer simulations. However they are complex to use, as such simulators are dedicated to differing design functions and not to impedance matching. Designers have to be familiar with the multiple data inputs that need to be entered and the correct formats. They also need the expertise to find the useful data among the various kinds of results coming out.

Alternatively a Smith chart may be used. Usage of a Smith chart allows impedance matching of complicated structures to be made without any computation. The only effort required is the reading and following of values along the circles. The Smith chart is a polar plot of the complex reflection coefficient. Examining the load where the impedance must be matched develops a Smith chart. Instead of considering its impedance directly, its reflection coefficient is employed to characterize a load.

3.4 The Driver

The active device will operate properly as a switch, as intended, if its input port is driven properly by the output of its driver stage. Most of the times driving constraints will also determine the upper limit for the frequency achievable.

The driver should provide enough “off” bias during the OFF interval to maintain the current through the switch acceptably small value. Similarly it should provide enough “on” drive during the ON interval to maintain a low enough “*Ron*” the resistance through the active device. Besides the driver should provide enough turn OFF fall-time, t_f, fast enough to make the turn-off power dissipation an acceptably small fraction of the output power and similarly should provide fast enough turn ON to make power dissipation during the turn-on switching acceptably small.

The input-port characteristics of BJTs, MOSFETs and MESFETs are completely different that a different driver circuit should be used for each type of transistors. However the scope of this thesis work is limited with MOSFETs.

The best gate-voltage drive is a trapezoid waveform, with the falling transition occupying 30% or less of the period. Shorter turn-off transition times yield less power dissipation in the output transistor during turn-off switching, but greater power consumption of the driver stage. The optimum drive minimizes the sum of the output-stage power dissipation and the driver-stage power consumption. The peak of the drive waveform should be safely below the MOSFET s maximum gate-source voltage rating. A sine wave is a usable but not optimum.

A MOSFET active device body possesses reactive properties attached. Of the great importance “the gate”, on which the drive signal to be applied will act as a high

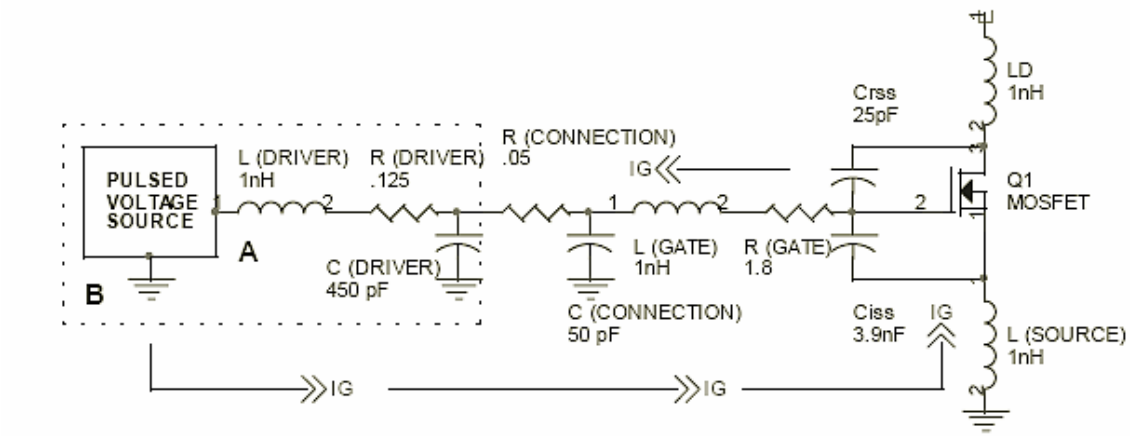

Fig 35. Gate input loop

value capacitor equivalent. Whereas other attached components introduce parasitic properties that inhibits the high-speed operation. The driver circuitry should essentially match this highly reactive and low impedance load to achieve proper driving.

The gate of a MOSFET possesses low impedance. On each of the RF cycle, this capacitor formed on the gate should be charged up to the necessary voltage and should be discharged. In fact, it is certainly impossible to load power into a purely

capacitive load. The power is necessary to be fed on to a resistor. This condition is supplied with resistor shunts and LC compensation.

Usually smaller MOSFETs or CMOS circuits on totem-pole arrangements are used. These are the various implementations of class-D and class-S operations. Several layout techniques and cascaded designs are employed to inhibit parasitic effects. Similarly transformers are exploited to drive this low impedance. However RF capable ferrite cores are required and the output is sinusoidal. Recently gate drive integrated circuits became popular. Only being fed with the desired frequency at TTL levels, these circuits are capable of driving MOSFETs with none of the other peripheral passive elements used.

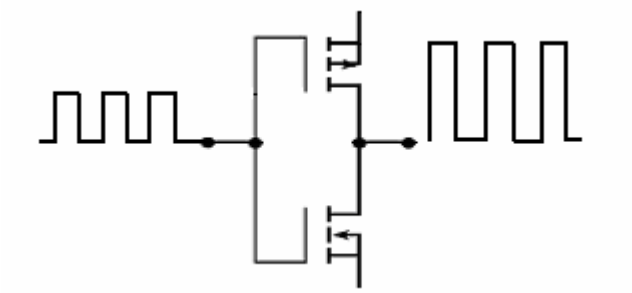

Fig 36. Totem-pole configuration

3.5 The Frequency Synthesizer

The operation frequency of the power generator is determined and controlled by a frequency synthesizer feeding the driver. Depended on the type of the driver employed and whether a frequency variation is required the frequency synthesizer is selected. For instance, the output signal type whether sinusoidal or square, the signal level and the source impedance. Totem-pole arrangement driver configurations and integrated circuit solutions will accept signal sources of the square wave type with acceptable fanouts on either TTL or CMOS levels. Whereas some others would require sine waves at lower voltages and buffer amplifiers should be used to supply lower impedances.

Apparently frequency synthesizer for the power generator of this thesis interest should refer crystal oscillators. They will provide the required stability. Further precautions might be taken against ambient variations such as NTC devices to have the crystal on a single certain temperature.

PLL circuits are more likely to be used as frequency synthesizers. Most of the times crystals for the desired frequency are not available since they are usually produced for communication purposes on allocated frequencies. Another reason is the possibility that the designer may wish the frequency synthesizer to supply signal at varying frequencies. This might be required for non-mechanical impedance matching or some other scientific research purposes.

A conventional PLL circuit possesses a voltage-controlled oscillator supplying the output signal. Besides it acquires a reference signal from another crystal oscillator. Both signals are continuously compared about their phase differences and an error signal is generated. After passing a low pass filter of either an active or a passive type, the error signal controls the voltage controlled oscillator.

Usually comparisons of two signals are conducted at a lower frequency and the output signal from the voltage-controlled oscillator is divided by a proper integer prior to phase comparison. Similarly the reference signal from the crystal oscillator may be exploited after a N-division. Simply altering these N dividend integers various frequencies are obtainable. At the time that the dividend integer is changed, usually with digital control, the frequency synthesizer will jump to a new predetermined frequency in milliseconds.

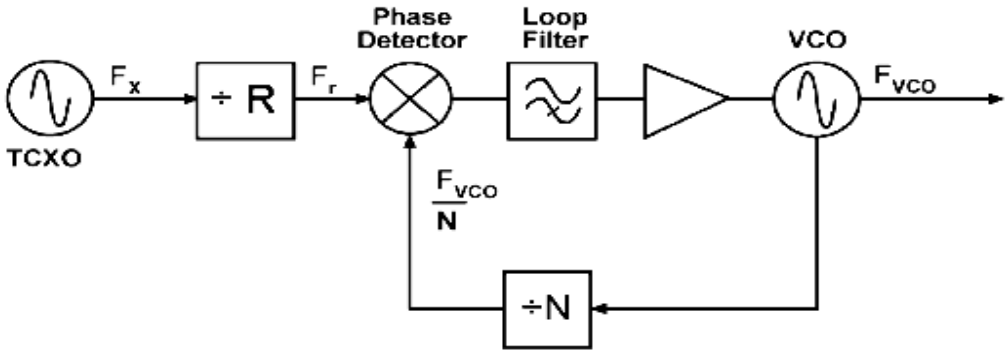

Fig 37. Classical Integer-N PLL block diagram

PLL circuits if correctly implemented are found to be extremely stable and useful. However without careful implementation conditions, especially for relatively lower comparison frequencies they are the sources of phase noises.

3.6 Power Conditioning

Generally speaking a power supply converting AC line voltage to DC power must perform the following functions at high efficiency and at low cost. It will provide rectification, converting the incoming AC line voltage to DC voltage. It will perform required voltage transformation and will supply the correct DC voltage level. It will provide a smooth the ripple of the rectified voltage. It will regulate the power so that the output voltage level will remain at a constant value irrespective of line, load and temperature changes. It will provide protection preventing damaging voltage surges from reaching the output; provide back-up power or shut down during a short circuit. Although providing isolation to electrically separate the output from the input voltage source should be considered as an absolute must, there exists some circumstances that isolation would not be necessary or performed previously with some other devices.

Discussions about the power conditioning requirements of the proposed device also covers issues on, adjustability from zero to the maximum, modulation, power factor correction, and electromagnetic interference.

These entire requirements may be satisfied with the usage of proper switching power supplies and filters. Besides with the usage of switching power supplies, the designer will be advantageous on device volume and weight issues. Switching power supplies are also capable of accepting power from all types of standard mains of both single or three phase, at various frequencies and voltages ignorant to the quality of signal provided. A single design is possible to be used with any mains all over the world.

A switch mode power supply, very much resembling the switch mode amplifiers of the previous discussions in take the DC or AC voltage at mains line frequency to convert it to a power of higher frequency varying from audio

frequencies to a few MHz. This power at high frequencies is than subject to voltage transformations on ferrite transformers, which are explicitly smaller in size and efficient. A supervisor circuit will in take the feedback from the output power, monitoring input and output voltages and current can provide regulation and modulation when necessary.

Out of many, together with buck and boost converters, full-bridge switch mode supplies are feasible of providing high power on the order of kilowatts to the proposed device. Half-bridge converters and flybacks would need huge transformers. Also buck and boost converters have other problems when used alone. They do not provide isolation, and remain insufficient when great differences between input and output voltages are necessary. However on many cases the system to be applied already employs a power conditioning system and usage of buck-boost converters will be sufficient. A boost converter will also be useful to be employed as PFC unit when used under control of a PFC integrated circuit.

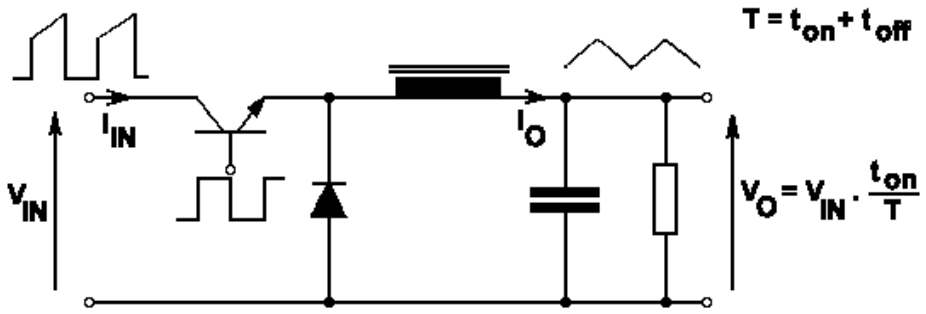

Fig 38. Buck Converter

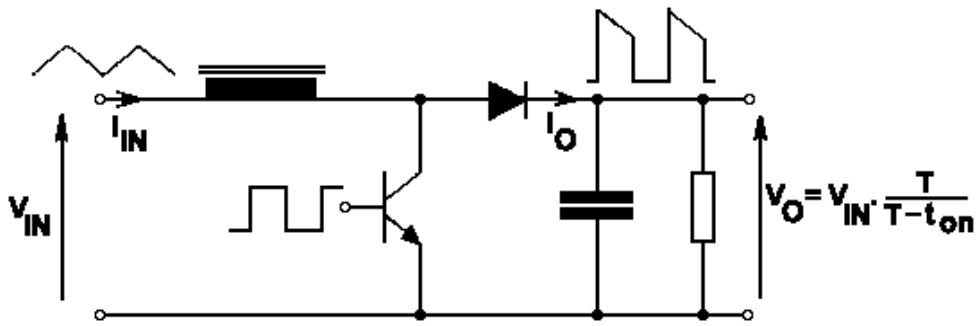

Fig 39. Boost Converter

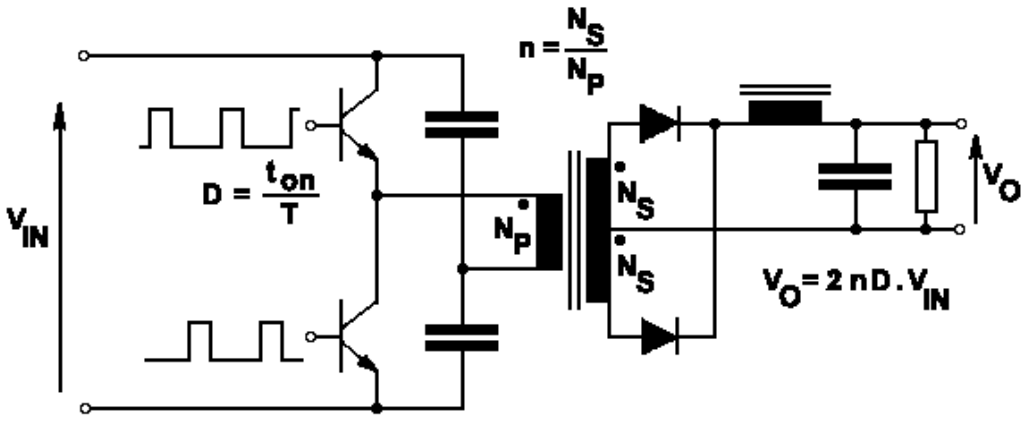

Fig 40. Half Bridge Converter

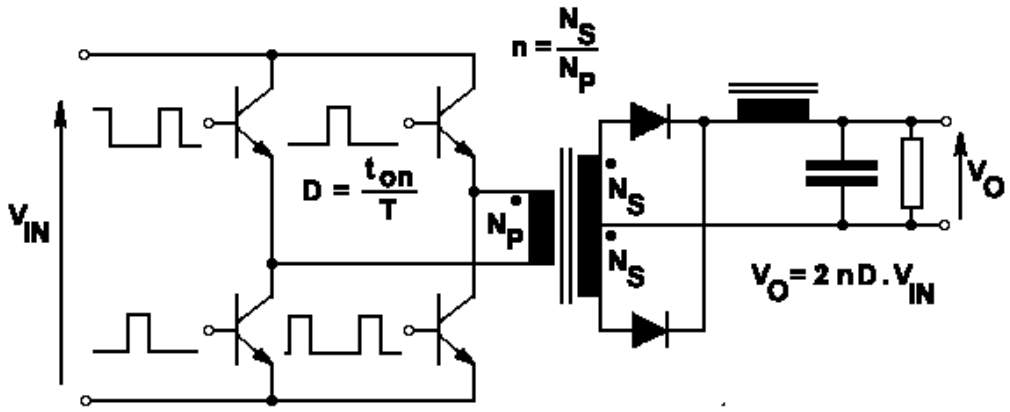

Fig 41. Full Bridge Converter

CHAPTER 4

IMPLEMENTATION
of the
PROPOSED SYSTEM

Among the implementation and experimental sessions, it would be a cleaver choice to stick on 13.56 MHz as the fundamental frequency. It is desirable to use an ISM frequency for demonstrative and legislative reasons. 13.56 MHz being as to be the lowest of these frequencies in the range of feasible ones for RF CCD applications. Immediately follows, for the fundamental frequency selected,

$$\omega = 2\pi\, 13.56\times 10^{6} \cong 85.12\times 10^{6}\, s^{-1} \tag{4.1}$$

$$T \cong 73.75 ns \tag{4.2}$$

$$\lambda \cong 22.11 m \tag{4.3}$$

4.1 Implemented Active Medium Characteristics

As mentioned earlier, this thesis work aims to implement the proposed device, primarily on to fast flow and slab CO2 lasers. Regarding the stability reasons these lasers are agreed to have their active medium not with a single pair of electrodes but a single electrode grounded and multiple electrode modules fed from the RF generator, supplying a segmented discharge among the active medium. By conducting implementations and experiments on a single one of these segmented

discharges, the designer will be able to foresee the over all capabilities and demands of the complete laser active medium.

As being subject to this thesis work three of such modules will be investigated. The first module is a small scale RF discharge experiment tool where experiments about the laser gas properties, lumped matching network element characteristics can be investigated and will provide intuitive information and experience about the nature of the RF discharge as well. This module has two disk electrodes each 0.8cm^2 with a 5mm gap between them. It also has gas inlets and outlets enabling the investigator to have gas flow during operation.

The second module is an exact replica of one of the 18 electrode segments of a slab CO2 laser that has been constructed to provide 600W of laser output. This electrode couple again is placed in vessel to provide vacuum conditions and laser gas flow. Rectangular electrodes each having an area of 50cm^2 is separated 9mm from each other.

Finally the third module will demonstrate the capabilities of the proposed device with fast flow designs. A Pyrex tube of 20mm in diameter having its electrodes outside the tube walls is used for this implementation. Electrodes are arranged in two configurations, on both of which they are not flat but their effective dielectric distance is estimated to be constant. One of these configurations has the electrode along with the tube with a proper curvature, intuitively aligned to provide constant field along tube dimensions. On the second arrangement electrodes are positioned around and along the tube with a spiral configuration. Effective electrode area will be 20cm^2 and the effective gap between electrodes is determined to be 20mm obviously.

These modules to be called A, B and C here after, also differs due to their dielectric properties. Module A possesses naked electrodes whereas the electrodes of module B are coated with 50 μm thick alumina. Module C will have its electrodes completely outside the discharge medium separated by Pyrex tube walls of 2mm thickness.

As it was noted earlier, prior to the ignition of the discharge the active medium will act as a capacitor. Following this phenomena, calculated dielectric specifications of each module at 13.56 MHz are tabulated on table 6.

Although varying pressure conditions are investigated as well, a certain pressure value to be held constant during numerical calculations and experimental implementations is decided. This value together with the pre-determined gap distance and field frequency forms a basis to discussions about the observations of discharge specifications depended on power generator capabilities and impedance matching issues. An elegant approach for the determination of a proper pressure value describing optimal RF excited CO_2 laser parameters is given on reference [9] due to similarity laws for RF discharges,

$$pd \approx 240 hPa.mm = 180 Torr.mm \tag{4.4}$$

$$fd \approx 280 MHz.mm \tag{4.5}$$

$$p/f \approx 0.86 hPa.MHz^{-1} = 0.645 Torr.MHz^{-1} \tag{4.6}$$

Although the equation (4.4) suggests 36, 20 and 9 Torr for setups A, B and C respectively, 12 Torr output of equation (4.6) will be selected since investigations are concentrated on power generator issues.

An approximate value for υ_c at 12 Torr is given to be 36 GHz [13]. The electron mobility term from equation (2.5) will yield μ_e=4.88$m^2V^{-1}s^{-1}$.

The plasma sheath thickness plays a very critical role on determination of active medium parameters as it was discussed on previous chapters. Effective sheath thickness was given with equation (2.12). This equation can be converted to a more plain term using electron mobility,

$$d_s = \frac{E_a \mu_e}{\omega} \tag{4.7}$$

which requires the knowledge of the strength of the applied field. However again reference [14] states a more elegant formula for optimal conditions,

$$d_s \approx 15 mm.MHz/f \tag{4.8}$$

which for the given frequency will yield a sheath thickness of 1.1mm.

The same formula (4.8), exploiting equation (4.7) will also inform us about an optimal applied field and applied voltage as well. Since the voltage applied will be the product of the applied field strength and the electrode gap, following voltages are found for modules A,B and C as 96V, 173V and 384V respectively.

In order to estimate the expectations from the purposed device, it should also be noted that, for the given frequency and gap distances maximum power densities are expected to appear between 1 to 10 $W.cm^{-3}$. However the maximum power density capabilities of the active medium as discussed previously, are directly related to excess heat removal considerations. A faster flowing of the gas mixture will allow higher power densities whereas increased gap distances will lower.

Module	**A**	**B**	**C**
Electrode Area (cm^2)	0.8	50	20
Gap Distance (mm)	5	9	20
Sheath thickness (mm)	1.1	1.1	1.1
Prior to Discharge Capacitance (pf)	0.14	4.92	0.89
Prior to Discharge Reactance (-jΩ)	84373	2400	13272
Post Discharge Capacitance (pf)	1.28	80.5	32.2
Post Discharge Reactance (-jΩ)	9228	146.7	366.8
Prior to Discharge LC match (μH)	996	28	157
Post Discharge LC match (μH)	109	1.7	4.4

Table 6. Reactive properties of experimental modules.

It is interesting to note the great differences of the reactance's of the active medium before and after ignition. Again module A, being of the small scale, in fact introduces more severe matching problems.

As a conclusion for the given set of modules, the power generator is responsible of supplying estimated figures of 400V applied voltage to the electrodes. Again followed by these figures and achievable power densities, the system is

required to match the load with the a resistance in the range of 10 to 600 and capable of resolving negative reactances from 100 to 500 jΩ.

Nevertheless, this requirement of adjustability on such a wide range of resistances and reactances may leave the idea of developing a single device possible to be used with various applications unfeasible, since introducing severe problems for the impedance matching solution. On the contrary an application specific device is required to be matched to a single reactance value, for instance -146.7 jΩ for the B module, allowing more plain impedance matching solutions. Similarly the plasma resistance will be expected on a much more narrow range.

4.2 Implementation of Class-E operation

Q_L being the free design parameter, basically, will be the trade of between the harmonic content and power capacity to be delivered to the active medium. Thus among the implementation of the class-E amplifier several values of Q_L in a range of 2 to 20 has been taken in to the account.

The MOSFET device "IXFH 6N100F" by IXYS Company decided to be utilized. This is the recommended device of IXYS to be used with RF discharge applications for being fast and capable of withstanding high powers. It is also noted to be convenient with switch mode applications. Absolute maximum ratings of this device are presented on table 7.

For being discussed on previous chapters, it should be noted that this device has the "$R_{ds\ on}$" figure of 1.9Ω when biased over the maximum threshold gate to source value of 5V. Consequently it will serve as a non-ideal switch of having 1.9Ω resistance while conducting.

Maximum voltage, maximum continuos current and maximum power dissipation capabilities of the device are the factors determining the design constraints of the class-E operation. Referring to equation (3.4) and table 7, with a safety factor of 0.9, "$V_{dd\ max}$" maximum DC voltage to be applied to the device is determined to be; 250V. As noted earlier, decreased applied DC voltage figures

would not affect other operation and design parameters severely but the output power. Hence 250V is to be taken to account for determination of maximum achievable power output.

Symbol	Test Conditions		Maximum Ratings	
V_{DSS}	T_J = 25°C to 150°C		1000	V
V_{DGR}	T_J = 25°C to 150°C; R_{GS} = 1 MΩ		1000	V
V_{GS}	Continuous		±20	V
V_{GSM}	Transient		±30	V
I_{D25}	T_C = 25°C		6	A
I_{DM}	T_C = 25°C, pulse width limited by T_{JM}		24	A
I_{AR}	T_C = 25°C		6	A
E_{AR}	T_C = 25°C		20	mJ
E_{AS}	T_C = 25°C		300	mJ
dv/dt	$I_S \le I_{DM}$, di/dt ≤ 100 A/μs, $V_{DD} \le V_{DSS}$ $T_J \le$ 150°C, R_G = 2 Ω		5	V/ns
P_D	T_C = 25°C		180	W
T_J			-55 ... +150	°C
T_{JM}			150	°C
T_{stg}			-55 ... +150	°C
T_L	1.6 mm (0.063 in.) from case for 10 s		300	°C
M_d	Mounting torque	TO-264	0.4/6	Nm/lb.in.
Weight		TO-247	6	g
		TO-264	4	g

Table 7. IXFH 6N100F device absolute maximum ratings [47].

Apart from the Q_L parameter, load resistance to be determined as a design choice referring, the maximum expected power, current capabilities of the device, maximum power dissipation of the device due to inefficient operation and misalignment circumstances and finally desired load resistance regarding the capabilities of the impedance matching network. Selection of 50 Ω might be another alternative since this source resistance impedance is the industry standard, and many

of the peripheral accessories, including commercial impedance matching networks are only available for this impedance rating.

Consequently with rather conservative selection of maximum operation parameters of the power generator, it has been decided to provide 720W of RF power on ideal 100% efficient conditions. These power ratings will allow a safe operation of the class-E operation with a peak current of 8.7A, which is well below the 21A given on table 7, unless the efficiency is kept over 75% and the heat sink is held at ambient temperatures. In fact, with the given MOSFET device a class-E amplifier is capable of delivering 1600W of RF power on ideal circumstances, however the difference with the power is sacrificed to remain conservative about safety factors.

Values for load network components and the shunt capacitance were evaluated referring to equations (3.12), (3.13) and (3.13). Nevertheless Q_L function components were omitted for the ease of calculations. Referring to equation (3.6) Q_L function is found to approach to unity in the order of Q_L values of 20. Lower Q_L values will have their effects on mostly the load resistance, decreasing its value slightly. In other words selection of decreasing values of Q_L lower than 20 will lead

Q_L	R load (Ω)	C1 (pf)	L2 (μH)	C2 (pf)
2	50	50	1.17	740
3	50	50	1.75	150
4	50	50	2.33	90
5	50	50	2.91	60
6	50	50	3.50	50
7	50	50	4.08	40
8	50	50	4.66	30
9	50	50	5.25	30
10	50	50	5.83	30
20	50	50	11.66	10

Table 8.Calculated passive component values.

to an increase on the output power. Nonetheless conservative values for the maximum power operation parameters are expected to compensate.

Finally DC feed choke is selected to be a commercial toroid inductor, capable of handling 6A.

Alternatively, equations for the class-E operation can be expressed to held a constant value for the quality factor of the loaded network and having a variable load resistance. A device which will co-operate with its attached power condition and impedance matching units to provide or to assist impedance matching requirements.

The amplifier supervisory circuit will mechanically adjust network load elements for the load they support for nominal conditions for a given QL value, and the DC voltage supply will follow these adjustments by varying the voltage applied to keep the power RF output stable. Nonetheless to be used with application specific devices where adjustments are required on narrower ranges, only to compensate for the system instabilities due to ambient variations, network elements can be electronically tuned. Active, voltage sensitive reactive components might be exploited in parallel with usual passive elements.

Similarly referring to publication [32], duty cycle ratio or the frequency of the input signal may be varied precisely by electronic means to be controlled on the driver. This will affect the load resistance supported by load network. Nevertheless such an alignment ill pay from the efficiency considerations, again to be compensated with the co-operation of the power regulator.

4.3 Implementation of Impedance Matching

As stated earlier, impedance matching needs for the desired application is remained within the resistive ranges of 10 to 600 Ω and negative reactances of 100 to 500 jΩ. The network will be asked to cancel this reactance by employing positive series reactance.

Several computer programs together with a Smith chart is utilized to perform calculations in order to satisfy impedance matching requirements of the proposed device. A Smith chart supports ease of usage, with out dealing with numerical

decisions. The parameters found are simply multiplied with desired quality factor. However a Smith chart will no more be feasible to be informed matching requirements of varying load. Same types of operations are necessary to be conducted many times repetitively. Most of the available computer software are application specific, only allowing limited types of operations or requiring knowledge of unnecessary parameters.

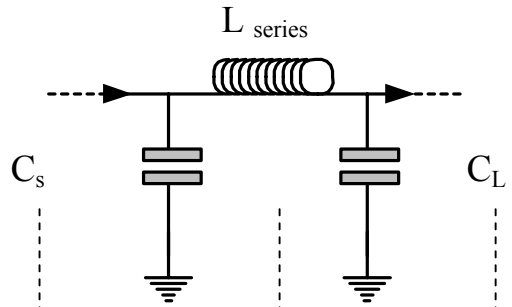

Load (Ω)	(pf)	(nH)	(pf)	Quality Factor
10-j100	704	1008	48	3
10-j100	938	938	99	4
10-j100	1174	674	150	5
10-j300	704	1303	84	3
10-j500	704	2040	50	3
100-j100	470	750	197	3
100-j300	470	1402	82	3
100-j500	470	2123	50	3
300-j100	191	1407	100	3
300-j300	191	1822	65	3
300-j500	191	2422	46	3
600-j100	151	1948	74	4
600-j300	151	2131	62	4
600-j500	151	2451	500	4

Table 9. Calculated matching network component values for various load impedance and quality factor conditions at 13.56 MHz.

Among investigations, one of these software [48] is found to be beautifully convenient about this thesis prospects. It allows the designer to simulate tuning and informs about the instantaneous voltage, current, power and phase angle parameters. However the software was inadequate to save the obtained data in useful forms. Each of one of the determined arrangements were necessary to be printed, whereas a better software should tabulate the obtained data in a useable format.

Initially it has been understood that, L- and T- type networks are not capable of satisfying these demands alone. As an example L type matching networks are necessary to be changed their order of reactive components regarding whether the load is higher or lower than 50Ω. Besides their operation will only be possible with higher values of quality factor, which will consequently cause the loss of power and ohmic heating of network elements. Else providing impedance matching with networks more than one is not consistent with reduced volume objectives of the proposed device.

Consequently, a Π-network is found to be a better solution capable of providing impedance match for a wider scale with very much lower quality factors of 2 or 3. Nonetheless even a Π-network will have problems, especially for values approaching 10Ω.

Outcomes of the calculations for impedance matching network elements worth discussions about several points. First, it should be noted that for a fixed value of resistive component of the load, reactive element C_s is held constant apparently observed from table 9. Second the quality factor is not necessarily an integer value.

Hence with minimal variations on the quality factor, for the load reactance held constant circumstances, it is promising to have other two elements constant but vary only a single reactive component to perform proper impedance matching. Although it is not as apparent as the first case, this can only be observed from table 9. That is, while quality factor and the reactive component held constant, C_L remained within acceptable limits.

Table 10 exhibits more obviously that, trends on component value adjustments possesses completely different characteristics over and bellow the source impedance of 50Ω.

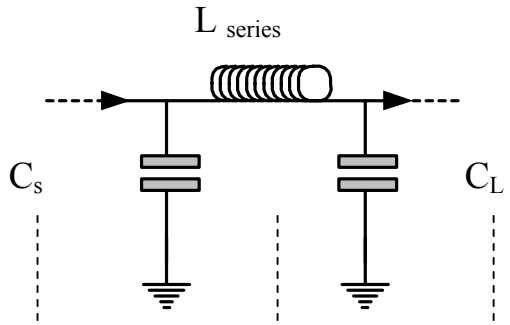

Load (Ω)	(pf)	(nH)	(pf)	Quality Factor
10-j147	704	1397	33	3
20-j147	704	1044	80	3
30-j147	704	892	114	3
40-j147	704	805	142	3
50-j147	704	749	166	3
60-j147	636	776	164	3
70-j147	581	802	160	3
80-j147	537	829	157	3
90-j147	501	856	154	3
100-j147	469	884	151	3

Table 10. Calculated matching network component values for module B at 13.56 MHz.

This knowledge states that a prudent selection of the load resistance introduced by the class-E operation will radically simplify the impedance matching requirements of the given application.

Following the above discussion, the matching system will possibly asked to assist more severe conditions when used with only one component variable. One of the major one is the period of pre-ignition power delivery. At this point it should be noted that, in fact after the power is applied, expected duration for the pre-ignition process would not be so long, that precautions should be taken. Reference [26] states that, when necessary amount of voltage is applied across the electrodes, the RF plasma will reach to its steady state conditions well before 50 RF cycles. 50 RF

cycles at 13.56 MHz would last for 3.7 μs. During this period only 2.7mW of power will be introduced into the system. Besides, in any case, the system would react after a much more longer period both by means of mechanical or electronic assistance.

Another discussion would be about the voltage fall followed by ignition period. The designer may need the steady state discharge conditions with an applied voltage level below the breakdown requirements of the active medium. This would especially be the case when the maximum voltage output of the generator should be limited due to some other constraints. This would require extra solutions to be employed on the matching system.

One of the other possible circumstances that would require further assistance of the matching unit will be the fault condition. As an example, a sudden loss of vacuum inside the active medium would lead to the loss of discharge and the matching unit will be asked to react.

A possible solution to these last questions is exhibited on figure 17, which is describing the proposed system. A RF relay will commute between two of the reactive components, for the position of the matching network balancing the negative reactance of the active medium.

4.4 Implementation of Driver

A detailed analysis is evaluated to determine the driving requirements of RF applications specific MOSFET very similar to IXFH 6N100F device is presented on the white paper of Directed Energy Inc. [46]. Results of this analysis were implemented to their circuit “FPS-4N”. Referring to this white paper a similar circuit is implemented.

The implemented circuit exploited IRFL110 surface mount MOSFET to form series of totem-pole arrangements. IRFL110 surface mount device is chosen for it is being cost effective, readily available, possible to be controlled on TTL logic levels and for being small enough to satisfy layout statements of reference [46].

This circuit was subject to a series of experiments, the most of which it is found to be capable of charging and de-charging the gate capacitance, 1870pf of

IXFH6N100F device to 18V at about 11ns. This performance is well enough to be used for 13.56 MHz where a period of RF cycle lasts 73.75ns.
Followed by these experiments a better alternative became commercially available. The "DEIC420" integrated circuit by Directed Energy Inc. is stated to be a "CMOS high speed high current gate driver specifically designed to drive MOSFETs in Class D and E HF RF applications at up to 45MHz" [49].

Trough rest of the experiments with class-E operation this device is employed, directly fed by the frequency synthesizer at TTL levels to drive the IXFH 6N100F device, requiring no other components but a by-pass capacitor.

4.5 Implementation of Frequency Synthesizer

The diagram exhibited on figure 18 implemented as the phase locked loop "PLL" frequency synthesizer of the proposed power generator. A pierce oscillator realized with logic inverter employing a 3 MHz crystal is used as the reference oscillator. This signal is divided by 25 to provide square wave oscillations at 120 kHz. 120 kHz was the best option to be obtained by commercially available crystals, which is a factor of 13.56 MHz. The highest possible factor was selected not to suffer from phase noise, when quality lacking passive low pass filter is implemented to the PLL circuit. An active filter was avoided not to increase the complexity of the system, especially since such a filters would require more sophisticated DC supplies.

Circuits designed with two different PLL integrated circuits. The first one was the 74HC4046 device by Philips Company. The constructed circuit was quite successful without any noticeable phase noise and frequency deviations. The disadvantage of the circuit was its relatively larger size compared to more modern equivalents. The circuit operation was limited with 17 MHz. Advantageously 74HC4046 device self contained a voltage controlled oscillator "VCO" and a design software was supplied. Of the greatest importance, this device guaranties a 50% duty cycle without any further precautions.

Alternatively a more modern circuit with surface mount components was constructed with TBB206 device by Siemens A.G.. TBB206 is self-contained

dividers for the reference and VCO signals. It has required a series data, in order to be informed about division factors and operation modes. Any operation is not possible with out this serial data supplied. This requirement made the circuit rather difficult to be implemented.

The circuit employing a 74HC4046 device is found to be satisfying for the proposed device. Exploiting advanced techniques and surface mount periphery circuits smaller dimensions are achievable. Series data input of the TBB206 device may be ambitious for future studies where a precise control over the operation frequency is desired. It should also be noted that a circuit employing the TBB206 device is necessary to have an 27.12 MHz output to be divided again back to 13.56 MHz in order to guarantee a 50% duty cycle.

CHAPTER 5

CONCLUSION and DISCUSSIONS

A very efficient, low cost and high power radio frequency power generator at 13.56 MHz ISM frequency was proposed to be exploited by RF excited CO_2 lasers, especially with diffusion cooled slab lasers with 400W to 800W optical outputs and fast flow lasers beyond 1kW.

A class-E amplifier in combination to a low pass filter to serve as an impedance matching tool intended to be used for the proposed system. 13.56 MHz chosen as the operating frequency, being a relatively lower frequency with in the ranges that the discharges of the desired form are obtainable. This frequency is allocated as being one of the ISM frequencies. Choice of a lower frequency made the design easier.

Class-E operation is desirable for it is being composed of a few numbers of components and it is probably the most efficient amplifier design for the frequency chosen. One should not only consider efficiency issue as maintenance costs but more important is that the heat removal problems and the capabilities of the active device to be used, that is how much power it can dissipate due to power loss. Compared to the class-A operation with the practical assumption of 30% efficiency, a 90% efficient class-E amplifier by using the same active device can deliver 21 times more power to the load. Besides it will be possible to operate it even with out a blower while conventional types of RF generators often need chiller units attached with the water flowing in.

In order to make a clear understanding of the demanded capabilities and unnecessary specification over which some savings are probable, active medium properties of CO_2 lasers and behavior of radio frequency discharges are investigated. Among the range of 200W to 1000W, moderate power CO_2 lasers have a number of important applications and some more to come in the near future. Trough this power range RF excited CO_2 lasers on slab configurations and exploiting unstable resonators seems to be outstripping other comparable equivalents.

Similar annular lasers, also exploiting RF excitation seems to be a promising competitor or successor candidates. Beyond 1kW of optical powers, RF excitation is again found to be a powerful tool to make laser designs more compact and more powerful. Besides combined operation of DC and RF discharges are also very useful at high powers against contraction phenomena. Waveguide lasers are another one of the type of CO_2 lasers, which are only feasible with RF excitation. Waveguide lasers are important for their application specific attractive properties.

RF excitation of active mediums of all fast flow, slab, waveguide and annular CO_2 lasers are understood to have optimum properties at moderate pressures 10-50 Torr, whereas of the usual practice RF excitation is achieved via capacitive coupling and various others like inductive or helicon are discarded and left for high pressures. However at moderate pressures capacitively coupled RF discharges, depended on the current density, have two different modes possessing obviously different characteristics at moderate pressures.

The α-mode discharges possess useful properties to excite the active medium of a CO_2 laser. With the γ-mode it is inefficient or even impossible to achieve a successful excitation. A possible exception, with the fast flow types of special geometry the designer may be ambitious to exploit sub-normal γ-modes or their simultaneous existence with α-modes.

It is pointed out that the plasma of a proper α-discharge resembles a network, which is composed with the series combination of a resistor and two capacitors. For the higher frequency ranges stray capacitance and inductance could also be accounted. Similarly prior to ignition, the resembling network is only a vacuum capacitor.

Ignition and maintenance of an α-discharge requires strict control of the voltage and current levels of the purposed device. An efficiently operating excitation system should not contain a power consuming ballast resistor to control the current flowing through the system. RF excitation allows usage of reactive components to serve as ballast resistors. Besides the proposed device should be capable of measuring and managing the amount current flowing accurately. It should be noted that the amount of current flowing is a combination of reactive and conduction currents. By the time before an excitation occurs it is only the reactive current flowing.

This last statement indicates another problem about the design of the proposed system, that is the desired properties of the current and voltage characteristics the system is different before and after the ignition. Also followed that this criterion will not necessarily be stable after ignition. These problems effects the load characteristics of the system requiring the impedance matching solution to be more complicated.

The load mismatch will result back reflection of the applied power and cause standing waves on the system. The system should generate solutions for the severe changes followed by ignition and plasma behavior during the maintenance period. The class-E operation is stated to be more tolerable against component imperfections or variations on component optimal values on several publications where the load seen by the amplifier is accounted to be a component value. However, in any case standing wave ratio should be observed during operation and immediate care should be taken. Intolerable levels of standing wave ratio will essentially cause damage on the active device and even on the passive components.

In order to increase this tolerance, the safety factor should be chosen to be higher through the determination of the DC feed of the amplifier, sacrificing the amount of obtainable power from each module and passive components should be selected of the lowest possible ESR types.

A possible solution to this last discussion is adjustable impedance matching system often used with practical applications. Since the harmonic content of the applied power is not one of the severe problems on a CO_2 laser application, a

relatively simple impedance matching circuit, a L-type or pi-type low pass filter with one or two capacitors and an inductor is exploited. The system is supposed to accomplish adjustments via variation of these components of the adjustable types or switching between a bunch of these components using relays and commutators.

However through the research made and the experiment carried out, these sorts of solutions are found to be unnecessarily complex, difficult to implement, of the high cost and voluminous. Besides even with the most rapid designs there are doubts about such mechanical matching network will react fast enough to protect a system reluctant to raise the safety factor, sacrificing obtainable power. In other words implementation of impedance matching boxes on to class-E systems are clearly understood to be in contradiction with the objectives of this thesis work.

Another approach to this problem comes from the idea just mentioned that the load seen by the amplifier is assumed to be a parameter of the operation. The system, in order to overcome the load mismatches, may adopt it self by continuously re-tuning other remaining parameters of the amplifier. In fact all other parameters and component values of a class-E system is dependent on the load seen and also with each other. Mechanical variation class-E amplifier passive components should again be considered unwillingly. Variation of; the DC feed voltage, the duty cycle of the driving signal, the frequency and usage of components which are tunable via electrical means are possible candidates.

The designer may also be ambitious to coat the electrodes of the active medium to be used with RF discharges with the dielectrics of the convenient type. Dielectric coatings of electrodes on RF discharges serve many purposes including the regulation of the discharge. Nonetheless, they have the property to elevate the optimum applied voltage level across the electrodes, which especially worth attention about the RF generator design, often aspiring since they support further current levels and consequently higher power outputs from a given active medium specifications. While proposing a RF excitation system covering an impedance matching solution, this issue should also be considered.

Similarly obtaining several times more power from a single module is seductive. Likewise provided that the device can withstand, referring to the direct

coupling conditions, it could be utilized on applications requiring higher voltages of several thousand volts. Thus, there is also a strong motivation to explore the proposed device with series and parallel operation of active devices.

Quality factor of the load network is a free to choose tool, affecting exactly all other parameters. Considering the trade of between a high and a lower Q_L levels, the designer should try to benefit from lower Q_L levels.

Through the research sessions, although some of the publications mentioned about dual frequency operations, plasma behavior with a series of field frequencies left unclear. Since lower Q_L levels of the load network results higher amounts of harmonic content, its effects on the plasma behavior would be useful information. Further research and experiments are necessary to understand the plasma conditions with multiple frequencies at various intensities are noted as a future study.

As it was mentioned earlier, an α-discharge can be assumed as a series network of capacitors and a resistor. Also regarding the previous discussion about measures to be taken against load mismatches, equivalent network elements of the α-discharge may be accounted as if they are absorbed into the series network components of the load network. A class-e amplifier directly coupled to the active medium, adopting it self to plasma impedance with the feedback information of the standing wave ratio is also left as novel solution to be studied on future.

A circuit similar to the PLL designs may be used to follow the phase difference between the voltage across the electrodes and the current flowing through, to probe the load mismatch conditions, to supply a feedback to the novel system mentioned. Once the effects of the increased harmonic content of the applied power to the plasma are known, mentioned novel device can be built with fever number of components similar to those proposed by N.O. Sokal [29]. Such a system will be substantially efficient, cost effective and compact satisfying all the objectives of this thesis work.

The research sessions stated that waveguide lasers are not possible at 13.56 MHz since the sheath thickness will be oversized compared to the cavity. Although the MOSFET demonstrated on this thesis work are not capable for operations over 30MHz, there are some other options, which are capable of operating at VHF

frequencies and still with relatively low costs. However these MOSFETs would not allow high voltages. In fact they are limited on a hundred volts. Followed by this work, now there is a strong motivation to design a system at lower voltages, operating at 81.36 MHz to be used with a waveguide design.

Apart from CO2 laser applications, such a device will be a desirable tool to be used with various other applications. Not only the capacitive components but also inductance may also be accounted as it is absorbed in to the load network. Consequently it will be possible to use this device with all forms of inductively coupled plasma and heating applications. Thus it can be concluded that, the proposed device and its novel improved version, which is left as a future work, are possible candidates to be used with all sorts of lasers exploiting RF excitation whereas they can be used with low pressure plasma applications of etching, deposition and ion implantation. Similarly various other applications such as RF heating are also possible.

REFERENCES

[1] Webster's Online Dictionary The Rosetta Edition™

[2] Javan A., Bennett W.R., Herriot D.R., Phys. Rev. Lett., Vol. 6, p. 106, 1961.

[3] Patel C.K.N., Phys. Rev. Lett., Vol.13, p.617, 1964.

[4] Brown C.O. and Davis J.W., Appl. Phys. Lett.,Vol. 21, p.480, 1972.

[5] He D. and Hall D. R., Appl. Phys. Lett., Vol. 43, p. 726, 1983.

[6] Polyani J. C., Jour. of Chem. and Phys., Vol. 34, (Jan., 1961) p.347

[7] Patel C.K.N., Phys. Rev. Lett., Vol.136, p.1187, 1964.

[8] Witteman W. J., The CO_2 Laser, Springer-Verlag, Berlin Heidelberg, 1987.

[9] Wieneke S., Uhrlandt C., Viöl W., Laser Phys. Lett.1, No. 5, p.241–247, 2004

[10] R. Nowack, K. Opower, H. Kruger, W. Haas, and N.Wenzel, Diffusion Cooled Compact CO2 high power lasers, Laser-Forschung, 1991.

[11] R. Nowack, K. Opower, H. Kruger, W. Haas, and N.Wenzel, Diffusion Cooled Compact CO2 High Power Lasers, Laser optoelectron., Vol. 23, p.68, 1991.

[12] Gutu I., Pascu M. L., New Design Of The High Power CO_2 Lasers for Industrial Applications, Bucharest 1992.

[13] Raizer Y. P., Shneider M. N., Yatsenko N. A., Radio-Frequency Capacitive Discharges, CRC Press, Boca Raton, 1995.

[14] Wieneke S., Born S., Viöl W.,J. Phys. D: Appl. Phys. Vol.30, p.1282-1286, 2000.

[15] Lieberman M. A. and Lichtenberg A. J., Principles of Plasma Discharges and Materials Processing, Wiley, New York, 1994.

[16] Brown S. C., Introduction to Electrical Discharges in Gases, John Wiley, NY,1966.

[17] Lieberman M. A., IEEE Trans. Plasma Sci. Vol.16, p. 638, 1988.

[18] Lieberman M. A., IEEE Trans. Plasma Sci. Vol.17, p. 338, 1989.

[19] Godyak V. A. and N. Sternberg, Phys. Rev. Vol. A 42, p. 2299, 1990.

[20] Sobolewski M. A., Appl. Phys. Lett. 70 (8), 1997

[21] LEOT, 3-8 Energy Transfer in Molecular Lasers, Center For Occupational Research and Development (CORD) in Texas, 2001

[22] Calvert J. B., Electrical Discharges, University of Denver

[23] Ganguli A. and Tarey R. D., Understanding plasma sources, Current Science, Vol. 83, No. 3, 2002

[24] Perret A. et. al., Ion Flux Uniformity In Large Area High Frequency Capacitive Discharges, UNAXIS, France

[25] Dine S. et. al., Coupled Power And Plasma Impedance Measurements In A VHF Capacitive Discharge In Hydrogen, Ecole Polytechnique, Palaiseau.

[26] Wester R. and Seiwert S., J. Phys. D: App. Phys. Vol.24, p.1371-1375, 1991.

[27] Wester R. and Loosen P., J. Phys. D: App. Phys. Vol.28, p.849-855, 1995.

[28] Sokal N.O., Class-E RF Power Amplifiers, p.9-20, QEX Jan/Feb 2001.

[29] Sokal N.O., IEEE J. S.S.C., Vol. SC-16, No. 4, 1981

[30] Tan L.S. and McMohan R.A., Power Electronics & V. S. D., No.429, IEEE, 1996.

[31] Raab F.H., IEEE J. S.S.C., Vol. SC-13, No. 2, 1978

[32] Kazimierczuk M.K. and Puczko K., IEEE Trans.C. S., Vol. CAS-34, No.2, 1987

[33] Collins D., Hinchliffe S. and Hobson L., Electronics Letters, Vol.23, No.18,1987

[34] Raab F.H.,IEEE Trans. C. S., Vol. CAS-24, No.12, 1977

[35] Sokal A.D. and Sokal N.O., IEEE J. S.S.C., Vol. SC-10, No. 3, 1975.

[36] Raab F.H. and Sokal N.O., IEEE J. S.S.C., Vol. SC-12, No. 1, 1977.

[37] Mandojana J.C. Herman K.J. and Zulinski R. E., IEEE Trans. C. S., Vol. CAS-37, No.8, 1990

[38] Rutledge D, et.al., High Efficiency Class-E Power Amplifiers, QST, May 1997.

[39] Krausse G.J., 1KW Class-E 13.56 MHz Single Device RF Generator for Industrial Applications, Directed Energy Inc. App Note, 2000.

[40] Frey R., Class-E 27.12 MHz Amplifier MOSFET, APT app. note APT9903

[41] Hinchliffe S. and Hobson L., Electronics Letters, Vol.24, No.14,1988

[42] Raab F.H, Sokal N.O et.al.,RF and Microwave Power Amplifier and Transmitter Technologies, High Frequency Electronics, May, 2003.

[43] Rutledge D. and Davis F. J., Industrial Class-E Amplifiers with Low-Cost Power MOSFETs and Sine-Wave Drive, RF Design,1997.

[44] Vania W. M.,PRF-1150 1KW 13.56 MHz Class-E RF Generator Evaluation Module, Directed Energy Inc. App Note,2002.

[45] Raab F.H, Sokal N.O, IEEE J. S.S.C., Vol. SC-13, No. 6, 1978.

[46] Krausse G.J., Gate Driver Design, Directed Energy Inc. App Note, 2001.

[47] IXFH 6N100F power MOSFET, Advanced Technical Information, IXYS, 2000.

[48] Tonne Match, Tonne J. L.,2001

[49] DEIC420 20 Ampere Low-Side Ultrafast RF MOSFET Driver, Directed Energy Inc. App Note, 2004.